Fractional Langevin equation: Overdamped, underdamped, and critical behaviors

S. Burov and E. Barkai
Department of Physics, Bar Ilan University, Ramat-Gan 52900, Israel

(Received 5 March 2008; revised manuscript received 14 May 2008; published 10 September 2008)

The dynamical phase diagram of the fractional Langevin equation is investigated for a harmonically bound particle. It is shown that critical exponents mark dynamical transitions in the behavior of the system. Four different critical exponents are found. (i) $\alpha_c=0.402\pm0.002$ marks a transition to a nonmonotonic underdamped phase, (ii) $\alpha_R=0.441\ldots$ marks a transition to a resonance phase when an external oscillating field drives the system, and (iii) $\alpha_{\chi_1}=0.527\ldots$ and (iv) $\alpha_{\chi_2}=0.707\ldots$ mark transitions to a double-peak phase of the "loss" when such an oscillating field present. As a physical explanation we present a cage effect, where the medium induces an elastic type of friction. Phase diagrams describing over and underdamped regimes, with or without resonances, show behaviors different from normal.

DOI: 10.1103/PhysRevE.78.031112 PACS number(s): 02.50.−r, 05.10.Gg, 05.70.Ln, 45.10.Hj

I. INTRODUCTION

In this paper we investigate the phenomenological description of stochastic processes using a fractional Langevin equation (FLE) [1–8]. While in simple systems the memory friction kernel is an exponentially decaying function or a δ function, in complex out-of-equilibrium systems the picture is in some cases different. Namely, the relaxation is of a power law type, and the particle may exhibit anomalous diffusion and relaxation [9]. Mathematically, such systems are modeled using fractional calculus, e.g., $\frac{d^{1/2}}{dt^{1/2}}$. An example is the recent experiment on protein dynamics of Xie and coworkers [10,11]. There anomalous dynamics of the coordinate x describing donor-acceptor distance was recorded, and a FLE (see Sec. II) was found to describe the experimental data. The motion of x is bounded by a harmonic force field, and the equation of motion for the average $\langle x\rangle$ is

$$\langle \ddot{x}\rangle + \omega^2\langle x\rangle + \gamma\frac{d^\alpha\langle x\rangle}{dt^\alpha} = 0, \tag{1}$$

where $0<\alpha<1$, ω is the harmonic frequency, and $\gamma>0$. For the case $\alpha=1$ we get the usual damped oscillator [12]. For such a normal case, two types of behavior, the underdamped and overdamped motions, are found. In the underdamped case $\langle x\rangle$ is oscillating and crossing the zero line, while for the overdamped case $\langle x\rangle$ is monotonically decaying with no zero crossing. For $\alpha=1$, there exists a critical frequency $\omega_c=\frac{\gamma}{2}$ that separates these two types of motion. Here we explore a similar scenario for the fractional oscillator, and find rich types of physical behaviors. It is known [13] that in the long-time limit all solutions $\langle x\rangle$ (i.e., for any $0<\alpha$, $0<\gamma$, and $0<\omega$) decay monotonically, somewhat like the overdamped behavior of the usual oscillator; however, now the decay is of power law type. The interesting physics occurs at shorter times where the solution may exhibit different types of relaxations and oscillations. We find that for $\alpha<\alpha_c$ the solution is nonmonotonic for any set of parameters $(\gamma,\omega>0)$. Thus we find a critical α that marks a dynamical transition in the behavior of the system.

We also investigate the response of a system described by Eq. (1) to an external oscillating force $F_0\cos(\Omega t)$. For the regular case of $\alpha=1$, a resonance is present if the frequency ω is larger than the critical value $\gamma/\sqrt{2}$. The behavior for $0<\alpha<1$ is quite different, and we discover that the transition between $\alpha\to1$ and $\alpha\to0$ is not smooth. In particular, we find another critical exponent α_R, where for $\alpha<\alpha_R$ a resonance is always present. Other critical exponents are found for the imaginary part of the complex susceptibility. Our goal is to clarify the nature of the solution to Eq. (1), investigate the meaning of the fractional critical frequency with and without external oscillating force, and provide a mathematical toolbox for finding and plotting solutions of Eq. (1). Our finding that critical α's mark dynamical transitions is very surprising and could not be obtained without our mathematical treatment.

The paper is organized as follows. In Sec. II we present the FLE. In Sec. III we present two different methods for solution and examples are solved in Sec. IV. In Sec. V we present different definitions for overdamped and underdamped motion and find the critical exponent α_c. We also interpret our results from a more physical point of view and discuss the cage effect as a viscoelastic property of the medium. In Sec. VI we introduce an external oscillating force into the system and find the response to such a force for free (Sec. VI A) and harmonically bound (Sec. VI B) particles. In Sec. VI C we investigate the properties of the "loss"—the imaginary part of the complex susceptibility. A summary is provided in Sec. VII, and the three Appendixes deal with some technical aspects. A brief summary of some of our results has been published [14].

II. THE MODEL

We consider the FLE

$$m\frac{d^2x(t)}{dt^2} + \bar{\gamma}\int_0^t \frac{1}{(t-t')^\alpha}\frac{dx}{dt'}dt' = F(x,t) + \xi(t), \tag{2}$$

where $\bar{\gamma}>0$ is a generalized friction constant $[\gamma=\frac{1}{m}\bar{\gamma}\,\Gamma(1-\alpha)]$, $0<\alpha<1$ is the fractional exponent, $\xi(t)$ is a stationary, fractional, Gaussian noise [15–17] satisfying the fluctuation-dissipation relation [18,19]

$$\langle \xi(t) \rangle = 0, \quad \langle \xi(t)\xi(t') \rangle = k_b T \bar{\gamma} |t - t'|^{-\alpha}, \tag{3}$$

and $F(x,t)$ is an external force. We follow the experiment [11] and assume $F(x,t) = -m\omega^2 x$; later in Sec. VI we will have $F(x,t) = -m\omega^2 x + F_0 \cos(\Omega t)$. In Laplace space it is easy to show, using the convolution theorem, that

$$\hat{x}(s) = \frac{s + (1/m)\beta(s)}{s^2 + (1/m)s\beta(s) + \omega^2} x_0 + \frac{1}{s^2 + (1/m)s\beta(s) + \omega^2} v_0 + \frac{1}{s^2 + (1/m)s\beta(s) + \omega^2} \xi(s), \tag{4}$$

where x_0 and v_0 are initial conditions and

$$\beta(s) = \bar{\gamma}\, \Gamma(1-\alpha) s^{\alpha - 1}. \tag{5}$$

Throughout this work, the variable in parentheses defines the space we are working in [e.g., $\hat{x}(s)$ is the Laplace transform of $x(t)$]. Equation (2) with $\alpha = \frac{1}{2}$ and $F(x,t) = -m\omega^2 x$ describes single-protein dynamics [11]. An experimentally measurable quantity is the normalized correlation function

$$C_x(t) = \frac{\langle x(t)x(0) \rangle}{\langle x(0)^2 \rangle}. \tag{6}$$

In what follows, thermal initial conditions are assumed, $\langle \xi(t)x(0) \rangle = 0$, $\langle x(0)^2 \rangle = k_b T / m\omega^2$, and $\langle x(0)v(0) \rangle = 0$. From Eq. (4) we find

$$\hat{C}_x(s) = \frac{s + \gamma s^{\alpha - 1}}{s^2 + \gamma s^{\alpha} + \omega^2}. \tag{7}$$

It is easy to show that $C_x(t)$ satisfies the following fractional equation:

$$\ddot{C}_x(t) + \omega^2 C_x(t) + \gamma \frac{d^{\alpha} C_x(t)}{dt^{\alpha}} = 0, \tag{8}$$

with the initial conditions $C_x(0) = 1$ and $\dot{C}_x(0) = 0$, where the fractional derivative is defined in the Caputo sense as [20,21]

$$\frac{d^{\alpha} f(t)}{dt^{\alpha}} = {}_0D_t^{\alpha - 1} \left(\frac{df(t)}{dt} \right) \tag{9}$$

and ${}_0D_t^{\alpha-1}$ is the Riemann-Liouville fractional operator [20,21]

$${}_0D_t^{\alpha - 1} f(t) = \frac{1}{\Gamma(1-\alpha)} \int_0^t (t - t)^{-\alpha} f(t) dt. \tag{10}$$

Note that another way to write Eq. (2) is

$$\ddot{x} + \gamma \frac{d^{\alpha} x}{dt^{\alpha}} + \omega^2 x = \xi(t); \tag{11}$$

hence the name fractional Langevin equation is justified. For a force-free particle [$F(x,t) = 0$ in Eq. (2)], $\langle x^2 \rangle \propto t^{\alpha}$ [7,22]; this is subdiffusive behavior since $0 < \alpha < 1$.

The FLE in general and Eq. (8) in particular can be derived from the Kac-Zwanzig model of a Brownian particle coupled to a harmonic bath [23]. The correlation function $C_x(t)$ as described by Eq. (8) can be derived also from the fractional Kramers equation [24]; however, the fractional Kramers equation does not correspond to a Gaussian process and the higher moments would differ from the FLE description. The use of fractional-differential equations like Eqs. (8) and (11) became quite common in recent years [9,25], for example in fields like fracture surfaces [26] and especially in the context of anomalous diffusion [9,27,28]. Several other fractional oscillator equations have been considered in the literature [29–31], and general solutions for fractional-differential equations of the type Eq. (8) have been studied in the mathematical literature [21,32,33]. In the next section we present a practical recipe, a toolbox, for the solution of Eq. (8), and show how to plot its solution. Our methods are general and can be applied to other linear fractional differential equations. From a more physical point of view the following questions are addressed in the next sections. (i) When is $C_x(t)$ positive (i.e., similar to overdamped behavior, $\alpha = 1$)? (ii) When is $C_x(t)$ nonmonotonic (similar to underdamped motion for $\alpha = 1$)? (iii) What is the analog to the critical frequency $\omega_c = \frac{\gamma}{2}$ found for the $\alpha = 1$ case? (iv) Does a critical exponent α_c exist, and if so what is its value?

III. THE GENERAL SOLUTION

In this section we will present a recipe for an analytical solution of Eq. (8). The formula for $C_x(t)$ in Laplace space is Eq. (7), and if α were an integer then it would be simple to perform an Inverse Laplace transform using analysis of poles [34,35], because then the denominator of Eq. (7) would be a polynomial. We assume α is of the form $\alpha = \frac{p}{q}$, where $q > p > 0$ are integers and $\frac{p}{q}$ is irreducible (i.e., not equal to some other $\frac{l}{n}$ where $l < p$ and $n < q$ are integers).

A. Method A

We rewrite Eq. (7) as

$$\hat{C}_x(s) = \frac{s + \gamma s^{p/q - 1}}{s^2 + \gamma s^{p/q} + \omega^2} \frac{\hat{Q}(s)}{\hat{Q}(s)} = \frac{(s + \gamma s^{p/q - 1})\hat{Q}(s)}{\hat{P}(s)}, \tag{12}$$

where $\hat{P}(s)$ is a polynomial in s. According to a mathematical theorem [21] we can always find $\hat{Q}(s)$ such that the denominator of Eq. (12),

$$\hat{P}(s) = (s^2 + \gamma s^{p/q} + \omega^2)\hat{Q}(s), \tag{13}$$

is a regular polynomial in s. The polynomial $\hat{Q}(s)$ is called the complementary polynomial. The task of finding $\hat{Q}(s)$ is simple: $\hat{Q}(s)$ is a polynomial in $s^{1/q}$ of degree $2q(q-1)$,

$$\hat{Q}(s) = \sum_{m=0}^{2q(q-1)} B_m s^{m/q} \tag{14}$$

with $B_{2q(q-1)} = 1$. The coefficients B_m are found by equating all the coefficients with noninteger powers of s in the expansion of the product $\hat{Q}(s)(s^2 + \gamma s^{p/q} + \omega^2)$ to zero. This produces a linear system of $2q(q-1)$ equations for $2q(q-1)$ variables, which in principle is a solvable problem.

We also assume that all $2q$ zeros of $\hat{P}(s)$ are distinct. The generalization to the case where the zeros are not distinct

will be treated later; such behavior is related to a critical frequency of the system. We use the partial fraction expansion

$$\frac{1}{\hat{P}(s)} = \sum_{k=1}^{2q} \frac{A_k}{s - a_k}, \tag{15}$$

where a_k are the solutions of $\hat{P}(s)=0$ and A_k are constants defined as

$$A_k = \frac{1}{\left.\frac{d\hat{P}(s)}{ds}\right|_{s=a_k}}. \tag{16}$$

It can be shown [21] that

$$\frac{s^m}{\hat{P}(s)} = \sum_{k=1}^{2q} \frac{a_k^m A_k}{s - a_k}, \quad m = 0,1,\ldots,2q-1. \tag{17}$$

The numerator of Eq. (12) is written using the expansion

$$\hat{Q}(s)(s + \gamma s^{p/q-1}) = \sum_{m=0}^{2q-1} \sum_{j=0}^{q-1} \tilde{B}_{mj} s^{m-j/q}. \tag{18}$$

Hence using Eqs. (12), (15), and (18)

$$\hat{C}_x(s) = \sum_{m=0}^{2q-1} \sum_{j=0}^{q-1} \sum_{k=1}^{2q} \frac{a_k^m \tilde{B}_{mj} A_k}{s - a_k} s^{-j/q}. \tag{19}$$

So finally we have reduced the problem of calculating the inverse Laplace transform of Eq. (7) to performing the inverse Laplace transform for

$$\frac{1}{s - a_k} \multimap\circ \quad e^{a_k t} \tag{20}$$

and

$$\frac{1}{s^{j/q}(s - a_k)} \multimap\circ \quad \frac{e^{a_k t}}{\Gamma\left(\frac{j}{q}\right) a_k^{j/q}} \gamma\left(\frac{j}{q}, a_k t\right), \tag{21}$$

where $\gamma(\frac{j}{q}, a_k t)$ is a tabulated incomplete gamma function [36] and $\hat{f}(s) \multimap\circ f(t)$ means that $\hat{f}(s)$ and $f(t)$ are Laplace pairs. Using the series expansion for $\gamma(a,x)$,

$$\gamma(a,x) = \Gamma(a) x^a e^{-x} \sum_{n=0}^{\infty} \frac{x^n}{\Gamma(a + n + 1)},$$

we can write Eq. (21) by means of the generalized Mittag-Leffler function [37]

$$\frac{1}{s^{j/q}(s - a_k)} \multimap\circ \quad t^{j/q} E_{1,1+j/q}(a_k t). \tag{22}$$

The Mittag-Leffler function satisfies

$$E_{\eta,\mu}(y) = \sum_{n=0}^{\infty} \frac{y^n}{\Gamma(\eta n + \mu)} \tag{23}$$

with

$$E_{\eta,\mu}(y) \sim -\frac{y^{-1}}{\Gamma(\mu - \eta)} y \to \infty. \tag{24}$$

To summarize, in order to perform the inverse Laplace transform of expressions like Eq. (7), we need to follow four steps. (i) Calculate $\hat{Q}(s)$, which is equivalent to the diagonalization of a matrix of size $[2q(q-1)]^2$. (ii) Find the zeros of $\hat{P}(s)$ and a_k, and the coefficients of the partial fraction expansion A_k of Eq. (16). (iii) Find the coefficients $\tilde{B}_{mj}$ for Eq. (18) and write $\hat{C}_x(s)$ as the sum in Eq. (19). (iv) Use Eqs. (20)–(22) to perform the inverse Laplace transform of Eq. (19). Finally, we find

$$C_x(t) = \sum_{m=0}^{2q-1} \sum_{j=0}^{q-1} \sum_{k=1}^{2q} \frac{a_k^{m-j/q} \tilde{B}_{mj} A_k e^{a_k t}}{\Gamma(j/q)} \gamma\left(\frac{j}{q}, a_k t\right), \tag{25}$$

where for $j=0$, $\gamma(\frac{j}{q}, a_k t)/\Gamma(\frac{j}{q}) = 1$, or using Eq. (22)

$$C_x(t) = \sum_{m=0}^{2q-1} \sum_{j=0}^{q-1} \sum_{k=1}^{2q} a_k^m \tilde{B}_{mj} A_k t^{j/q} E_{1,1+j/q}(a_k t) \tag{26}$$

and for $j=0$ $E_{1,1+j/q}(a_k t) = e^{a_k t}$. Now we have a practical tool for finding an explicit analytical solution for the fractional damped harmonic oscillator. Since $\gamma(a,x)$ is tabulated in programs like MATHEMATICA, the solution, which is a finite sum of such incomplete gamma functions, can be plotted.

B. Method B

The task of finding $\hat{Q}(s)$ is sometimes difficult since, as described in Sec. III A, generally one must solve a linear system of $2q(q-1)$ equations with $2q(q-1)$ variables. But for the special case of Eq. (7) we will provide a simple method for finding $\hat{Q}(s)$ and $\hat{P}(s)$. By writing

$$C_x(t) = \frac{s + \gamma s^{p/q-1}}{(s^2 + \omega^2)^q + (-1)^{q-1} \gamma^q s^p} \left(\frac{(s^2 + \omega^2)^q + (-1)^{q-1} \gamma^q s^p}{s^2 + \gamma s^{p/q} + \omega^2} \right), \tag{27}$$

we can write

$$\hat{Q}(s) = \frac{(s^2 + w^2)^q + (-1)^{q-1} \gamma^q s^p}{s^2 + \gamma s^{p/q} + w^2} \tag{28}$$

and

$$\hat{P}(s) = (s^2 + \gamma s^{p/q} + w^2)\hat{Q}(s) = (s^2 + \omega^2)^q + (-1)^{q-1} \gamma^q s^p. \tag{29}$$

One easily sees that indeed $\hat{P}(s)$ is a polynomial in s. As for $\hat{Q}(s)$, it is found by the standard method of division of two polynomials in $s^{1/q}$ and it is also a polynomial in $s^{1/q}$. Since the fraction of two polynomials

$$\frac{(y^{2q} + \omega^2)^q + (-1)^{q-1} \gamma^q y^{qp}}{y^{2q} + \gamma y^p + \omega^2} \tag{30}$$

is also a polynomial in y, we see that any solution of $y^{2q} + \gamma y^p + \omega^2 = 0$ is also a solution of $(y^{2q} + w^2)^q + (-1)^{q-1} \gamma^q y^{qp}$

=0, and by performing the substitution $y=s^{1/q}$ into Eq. (30) we find that indeed $\hat{Q}(s)$ is a polynomial in $s^{1/q}$. After finding $\hat{Q}(s)$ and $\hat{P}(s)$ explicitly, we can return to method A and use Eqs. (15)–(26) in order to write down the final solution.

IV. EXAMPLES $\alpha=1/2$ AND $\alpha=3/4$

A. $\alpha=1/2$

The $\alpha=\frac{1}{2}$ case was recently measured in experiment [11], and so it will be our first illustration for the method. From Eq. (7) we get

$$\hat{C}_x(s) = \frac{s+\gamma s^{-1/2}}{s^2+\gamma s^{1/2}+\omega^2}. \tag{31}$$

The first step is to find the complementary polynomial of the denominator on the right-hand side of Eq. (31). Using method A of the previous section, one can easily see that the coefficients of the complementary polynomial $\hat{Q}(s)$ are

$$B_4=1, \quad B_3=B_2=0, \quad B_1=-\gamma, \quad B_0=\omega^2$$

and

$$\hat{Q}(s) = s^2-\gamma s^{1/2}+\omega^2, \tag{32}$$

since

$$\hat{P}(s) = \hat{Q}(s)(s^2+\gamma s^{1/2}+\omega^2) = s^4+2\omega^2 s^2-\gamma^2 s+\omega^4. \tag{33}$$

We rewrite Eq. (31) as

$$\hat{C}_x(s) = \frac{s^3+s\omega^2-\gamma^2+\gamma\omega^2 s^{-1/2}}{(s^2+\omega^2)^2-\gamma^2 s} \tag{34}$$

and notice that the degree of the denominator of Eq. (34), i.e., $\hat{P}(s)$, is 4. Its zeros are easily found using the Ferrari formula [36], and we call them a_k, $k=1,\ldots,4$. The coefficients of the partial fraction expansion A_k are given by Eq. (16),

$$A_k = \frac{1}{4a_k(a_k^2+\omega^2)-\gamma^2}. \tag{35}$$

The partial fraction expansion is found using Eq. (19),

$$\hat{C}_x(s) = \sum_{m=0}^{3}\sum_{j=0}^{1}\sum_{k=1}^{4} \frac{a_k^m \widetilde{B}_{mj} A_k}{s-a_k} s^{-j/q}, \tag{36}$$

and the $\widetilde{B}_{mj}$ in Eq. (18) are found using the numerator of Eq. (34),

$$\widetilde{B}_{30}=1, \quad \widetilde{B}_{10}=\omega^2, \quad \widetilde{B}_{00}=-\gamma^2, \quad \widetilde{B}_{01}=\gamma\omega^2. \tag{37}$$

The other elements of the matrix $\widetilde{B}_{mj}$ are equal to 0. Using Eq. (25) the solution is

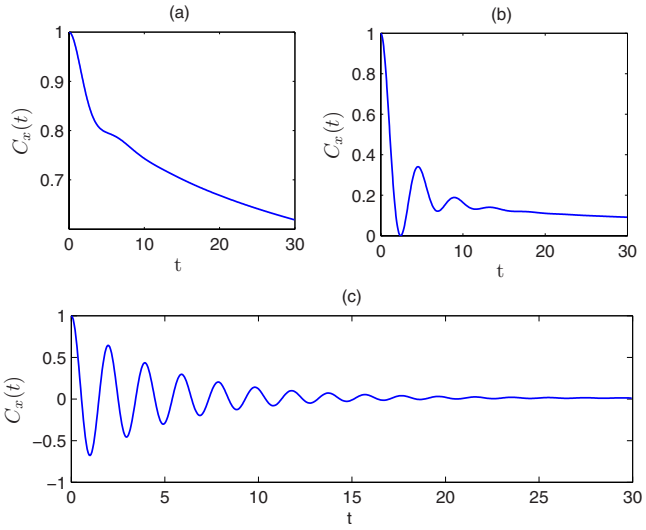

FIG. 1. (Color online) Short-time behavior for $C_x(t)$ with $\alpha=1/2$ and $\gamma=1$, versus t. Three types of solutions are presented: (a) $\omega=0.3$ and the function decays monotonically; (b) $\omega=\omega_z\approx 1.053$, the transition between motion with and without zero crossing, $C_x(t)=0$ at a single point in time, and $C_x(t)$ does not cross the zero line; (c) $\omega=3$, the underdamped regime. Note that, for large t, $C_x(t)>0$.

$$C_x(t) = \sum_{k=1}^{4}[(-\gamma^2+\omega^2 a_k+a_k^3)A_k e^{a_k t}+\gamma\omega^2 A_k t^{1/2}E_{1,3/2}(a_k t)]. \tag{38}$$

By using a series expansion and some algebra we find a_k, and Eq. (38) has the following asymptotic behavior:

$$C_x(t) = \begin{cases} 1-\frac{1}{2}\omega^2 t^2+\frac{\gamma\omega^2}{\Gamma\left(\frac{9}{2}\right)}t^{7/2}, & t\to 0, \\ \frac{\gamma}{\omega^2\Gamma\left(\frac{1}{2}\right)}t^{-1/2}-\left(\frac{\gamma}{\omega^2}\right)^3\frac{t^{-3/2}}{2\Gamma\left(\frac{1}{2}\right)}, & t\to\infty. \end{cases} \tag{39}$$

We see that $C_x(t)$ for long times decays as a power law, which is the signature of slow relaxation and anomalous diffusion. The same asymptotic results are found by applying Tauberian theorems [38] to Eq. (31).

The asymptotic expansion Eq. (39) provides the behavior for long (and short) times, but the intermediate behavior is not obvious. Using the exact solution Eq. (38) we plot $C_x(t)$ for various values of ω in Fig. 1. Three types of behavior exist: (i) Monotonic decay of the solution—Fig. 1(a); (ii) nonmonotonic decay in the non-negative half of the plane $C_x(t)\geq 0$—Fig. 1(b); and (iii) oscillations of the solution, where $C_x(t)$ also takes negative values—Fig. 1(c). These are typical behaviors of the solution which we found also in other parameter sets (not shown). From Fig. 1 we identify $\omega=\omega_z=1.053$ as a fractional critical point, in the sense that if $\omega>\omega_z$ we have zero crossings for $C_x(t)$. For $\alpha=\frac{1}{2}$ there exists also another fractional critical point $\omega_m=0.426$ where for $\omega<\omega_m$ $C_x(t)$ is monotonically decaying—Fig. 1(a). We will soon discuss ω_z and ω_m more generally.

B. $\alpha=3/4$

In this section we demonstrate the solution for $\alpha=\frac{3}{4}$ using method B. Our goal is to invert Eq. (7),

$$\hat{C}_x(s)=\frac{s+\gamma s^{3/4-1}}{s^2+\gamma s^{3/4}+w^2}. \tag{40}$$

We find the complementary polynomials $\hat{Q}(s)$ and $\hat{P}(s)$, using Eqs. (28) and (29),

$$\hat{P}(s)=(s^2+\omega^2)^4-\gamma^4 s^3 \tag{41}$$

and

$$\begin{aligned}\hat{Q}(s)&=\frac{(s^2+\omega^2)^4-\gamma^4 s^3}{s^2+\gamma s^{3/4}+\omega^2}\\&=s^6-\gamma s^{19/4}+3\omega^2 s^4+\gamma^2 s^{7/2}-2\omega^2\gamma s^{11/4}-\gamma^3 s^{9/4}\\&\quad+3\omega^4 s^2+\omega^2\gamma^2 s^{3/2}-\gamma\omega^4 s^{3/4}+\omega^6,\end{aligned} \tag{42}$$

and so we can write Eq. (40) as

$$\hat{C}_x(s)=\frac{s^7+3\omega^2 s^5+\gamma\omega^2 s^{15/4}+3\omega^4 s^3-\gamma^2\omega^2 s^{5/2}-\gamma^4 s^2+2\gamma\omega^4 s^{7/4}+\gamma^3\omega^2 s^{5/4}+\omega^6 s-\gamma^2\omega^4 s^{1/2}+\gamma\omega^6 s^{-1/4}}{(s^2+\omega^2)^4-\gamma^4 s^3}. \tag{43}$$

The degree of the denominator of Eq. (43) is 8, so the zeros of the polynomial $\hat{P}(s)$ could only be found numerically using a program like MATHEMATICA. As in the previous section, we call the zeros of $\hat{P}(s)$ a_k, $k=1,\ldots,8$, and the coefficients of the partial fraction expansion A_k are found using Eq. (16),

$$A_k=\frac{1}{8a_k(a_k^2+\omega^2)^3-3\gamma^4 a_k^2}. \tag{44}$$

Writing the partial fraction expansion using Eq. (19),

$$\hat{C}_x(s)=\sum_{m=0}^{7}\sum_{j=0}^{3}\sum_{k=1}^{8}\frac{a_k^m\tilde{B}_{mj}A_k}{s-a_k}s^{-j/q}, \tag{45}$$

where the coefficients $\tilde{B}_{mj}$ are found using the numerator of Eq. (43),

$$\tilde{B}=\begin{pmatrix}0&\gamma\omega^6&0&0\\ \omega^6&0&-\gamma^2\omega^4&0\\ -\gamma^4&2\gamma\omega^4&0&\gamma^3\omega^2\\ 3\omega^4&0&-\gamma^2\omega^2&0\\ 0&\gamma\omega^2&0&0\\ 3\omega^2&0&0&0\\ 0&0&0&0\\ 1&0&0&0\end{pmatrix}. \tag{46}$$

Using Eq. (25) the solution is

$$\begin{aligned}C_x(t)&=\sum_{k=1}^{8}A_k e^{a_k t}(a_k\omega^6-a_k^2\gamma^4+3a_k^3\omega^4+3a_k^5\omega^2+a_k^7)\\&\quad+A_k e^{a_k t}\left(\frac{\gamma\gamma\left(\frac{1}{4},a_k t\right)}{\Gamma\left(\frac{1}{4}\right)}(\omega^6 a_k^{-1/4}+2\omega^4 a_k^{7/4}+\omega^2 a_k^{15/4})\right.\\&\quad\left.+\frac{\gamma^2\gamma\left(\frac{1}{2},a_k t\right)}{\Gamma\left(\frac{1}{2}\right)}(\omega^4 a_k^{1/2}+\omega^2 a_k^{5/2})+\frac{\omega^2 a_k^{5/4}\gamma^3\gamma\left(\frac{3}{4},a_k t\right)}{\Gamma\left(\frac{3}{4}\right)}\right),\end{aligned} \tag{47}$$

or using Eq. (26)

$$\begin{aligned}C_x(t)&=\sum_{k=1}^{8}A_k e^{a_k t}(a_k\omega^6-a_k^2\gamma^4+3a_k^3\omega^4+3a_k^5\omega^2+a_k^7)\\&\quad+A_k[\gamma t^{1/4}E_{1,5/4}(a_k t)(\omega^6+2\omega^4 a_k^2+\omega^2 a_k^4)\\&\quad+\gamma^2 t^{1/2}E_{1,3/2}(a_k t)(\omega^4 a_k+\omega^2 a_k^3)\\&\quad+\omega^2 a_k^2 t^{3/4}\gamma^3 E_{1,7/4}(a_k t)].\end{aligned} \tag{48}$$

The behavior described by Eq. (48) is plotted in Fig. 2. Three typical types of behavior are shown, which are similar to the behavior for the $\alpha=\frac{1}{2}$ case (Fig. 1). The values of critical points for $\alpha=\frac{3}{4}$ are $\omega_m\approx 0.707$ [and so for $\omega=0.3$ we observe in Fig. 2(a) a monotonic decay] and $\omega_z\approx 0.965$, a case plotted in Fig. 2(b). Finally the case $\alpha=\frac{1}{5}$ is shown in Fig. 3. The difference between $\alpha=\frac{1}{5}$ and the former cases is that for $\alpha=\frac{1}{5}$ $\omega_m=0$ and so we never observe a monotonic decay of the solution. More generally, this behavior is obtained for any $\alpha<\alpha_c\simeq 0.402$, as we shall soon show.

V. DEFINITION OF OVER AND UNDERDAMPED MOTION

As mentioned in the introduction, when dealing with the normal damped oscillator one gets two types of solutions—overdamped and underdamped, the transition between these two behaviors happens at some point ω_c called the critical

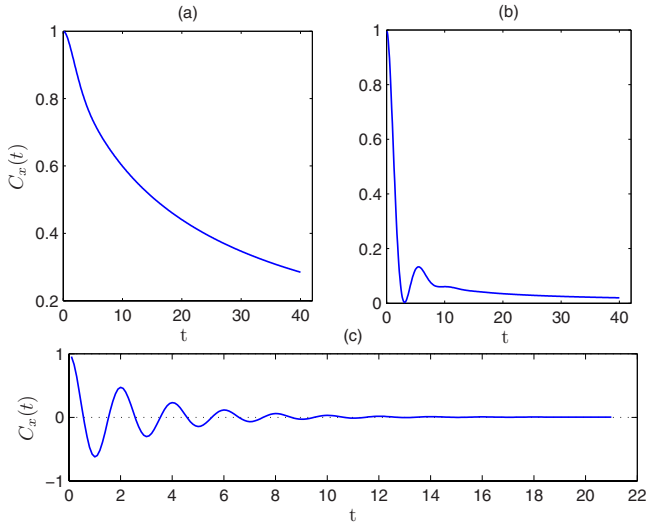

FIG. 2. (Color online) Short-time behavior for $C_x(t)$ with $\alpha=3/4$ and $\gamma=1$, versus t. Three types of solutions are presented: (a) $\omega=0.3$ and the function decays monotonically; (b) $\omega=\omega_z\approx 0.965$, the transition between motion with and without zero crossing, $C_x(t)$ does not cross the zero line; (c) $\omega=3$, the underdamped regime.

point. For the overdamped motion $\langle x\rangle>0$ for any t when $\langle x(t=0)\rangle>0$, and there are no oscillations, and for the underdamped case $\langle x(t)\rangle$ oscillates and crosses the zero line. For the fractional oscillator, we notice that there are different types of behaviors. From Figs. 1–3 one notices that for short times there is an oscillating behavior either with and without zero-crossings or a monotonic decay type of behavior. So as in the regular damped oscillator we need to define the transition between these behaviors. We propose three definitions for the point of transition between overdamped and underdamped motions, these are based on the various definitions that exist for the regular damped oscillator and give the same result for $\alpha=1$. The first option is to take the frequency ω_c for which two solutions of $\hat{P}(s)=0$ coincide, i.e., an appearance of a pole of a second order for $\hat{C}_x(s)$, and the general solution of Sec. III must be modified, as explained in Appendix A. The second option is to take the minimal frequency ω_z at which the solution $C_x(t)$ crosses the zero line and the third is to take the minimal frequency ω_m at which $\frac{dC_x(t)}{dt}$ crosses the zero line (i.e., $C_x(t)$ is no longer a monotonically decaying function). For regular damped oscillator $\omega_c=\omega_z=\omega_m$, but in fractional case this is generally not true.

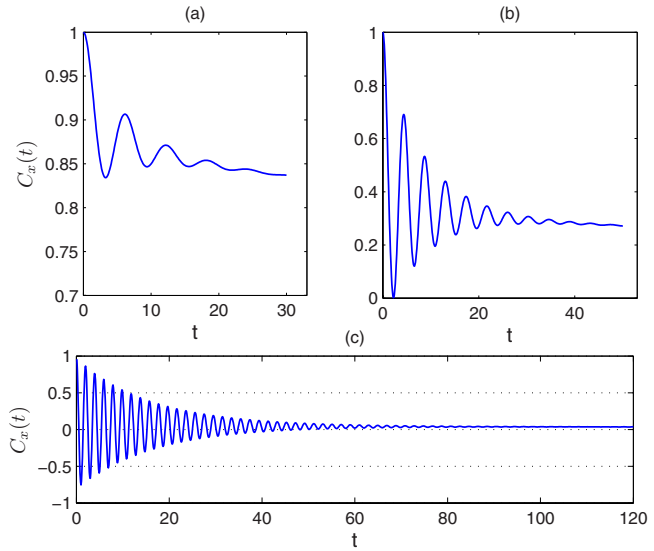

FIG. 3. (Color online) Short-time behavior for $C_x(t)$ with $\alpha=1/5$ and $\gamma=1$, versus t. Three types of solutions are presented: (a) $\omega=0.3$ and the function oscillates above zero; (b) $\omega=\omega_z=1.035$, the transition between motion with and without zero crossing, $C_x(t)$ does not cross the zero line; (c) $\omega=3$, oscillations with zero crossing for short times; for long times $C_x(t)>0$ and no oscillations are observed. For this case solutions with monotonic decay are not found since $\alpha=1/5<\alpha_c=0.402$.

Another difference between the fractional oscillator and the regular one is the distinction between short and long time behavior when $0<\alpha<1$. The asymptotic behavior for general α is obtained using general properties of polynomial solutions [21] with Eq. (23) and Eq. (24) or using the Tauberian theorem [38]

$$C_x(t)\approx 1-\frac{1}{2}\omega^2t^2+\frac{\omega^2\gamma}{\Gamma(5-\alpha)}t^{4-\alpha}\quad t\to 0 \tag{49}$$

$$C_x(t)\approx\frac{\gamma}{\omega^2\Gamma(1-\alpha)}t^{-\alpha}\quad t\to\infty \tag{50}$$

where the large t expression was obtained in [11,13,17]. The applicability of Eq. (50) is possible only under two conditions, the first one is obvious from Eq. (50) and is

$$\left(\frac{\omega^2}{\gamma}\right)^{1/\alpha}t\gg 1, \tag{51}$$

while the second is

$$|a|t\gg 1, \tag{52}$$

where $|a|$ is an absolute value of a zero of the enumerator in Eq. (7) $(s^2+\gamma s^\alpha+\omega^2)$, it also could be found from $\hat{P}(s)=0$. Mathematically the second condition is the magnitude of the radius of convergence for the power series expansion of $\hat{C}_x(s)$ near $s=0$ (Tauberian Theorem), and is given by the non-fictitious poles of $\hat{C}_x(s)$. From Eq. (50), $C_x(t)>0$ and for large t it decays as a power-law.

From a more physical point of view, the FLE formalism was used [11] to describe the fluctuation of the distance between a fluorescein-tyrosine pair within a single protein on a time scales of 1 msec up to 10^2 sec, and a power-law decay was observed (lately a theoretical model of Fractons was proposed in order to explain such phenomena [44]). Recent molecular dynamics simulations [45] studied the fluctuations of a donor-acceptor distance for a single protein, for short time scales 10^{-9} sec and oscillations of the autocorrelation function were observed. The scenario of oscillations for short-times and a power-law decay for long-times sets well with the description by our solutions of the FLE.

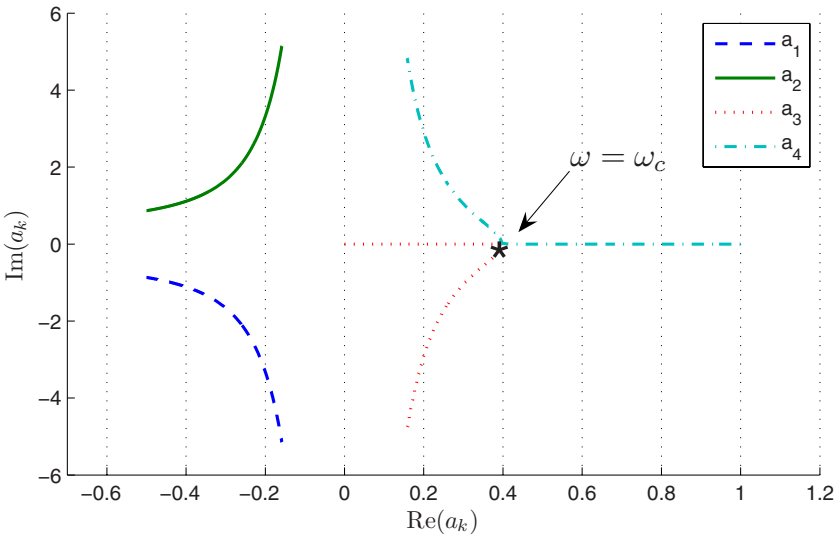

FIG. 4. (Color online) Four solutions of $\hat{P}(a_k)=0$ in the imaginary plane for $\alpha=1/2$, $\gamma=1$, and $0<\omega<5$. At the critical point $\omega=\omega_c=0.6873$ we have $a_3=a_4$.

A. Critical point ω_c

For the case $\alpha=\frac{1}{2}$ we have four solutions for $\hat{P}(s)=0$ (a_k $k=1,\ldots,4$) which are plotted in Fig. 4. At one point two solutions coincide, we call this point the critical point at which $\omega=\omega_c$. For $\omega=\omega_c$, the solution for $C_x(t)$ Eq. (38) must be modified because our general method derived Sec. III is not valid. For $\alpha=\frac{1}{2}$ and $\omega=\omega_c=\frac{1}{2^{2/3}}\sqrt{(3/2)(1/2)^{1/3}}\gamma^{2/3}$ [see Eq. (59)] Eq. (38) is [see Appendix, Eq. (A11)]

$$C_x(t)=\sum_{m=0}^{3}\sum_{j=0}^{1}\widetilde{B}_{mj}t^{j/2}\left[\sum_{k=1}^{3}a_k^m A_k E_{1,1+\frac{j}{2}}(a_k t)+a_3^m\widetilde{A}\times\left((t+ma_3^{-1})E_{1,1+j/2}(a_3 t)-\frac{j}{2}tE_{1,2+j/2}(a_3 t)\right)\right] \tag{53}$$

where $a_1\neq a_2\neq a_3$ and $a_4=a_3$ are zeros of $\hat{P}(s)$ given by Eq. (33), $\widetilde{B}_{mj}$ are found using Eq. (37), A_1 and A_2 by Eq. (35), $A_3=-(A_1+A_2)$ by Eq. (87) and $\widetilde{A}$ is defined in Eq. (88).

We emphasize that the critical point ω_c does not always exist. In Fig. 5 we plot the 10 solutions of $\hat{P}(s)=0$ for $\alpha=\frac{2}{5}$, and demonstrate that no two solutions coincide. We will soon show that for any odd q and even p the critical point ω_c does not exist.

Mathematically at critical points one of the coefficients of partial fractions expansion, A_k in Eq. (16), diverges. This happens because when two a_k coincide, $\hat{P}(s)$ can be written as $(s-a_k)^2\hat{G}(s)$, where $\hat{G}(s)$ is some polynomial in s and $G(a_k)\neq 0$, and

$$A_k=\frac{1}{\left(2(s-a_k)\hat{G}(s)+(s-a_k)^2\dfrac{d\hat{G}(s)}{ds}\right)\Big|_{s=a_k}} \tag{54}$$

diverges. And so in order to find such critical point two conditions must be satisfied

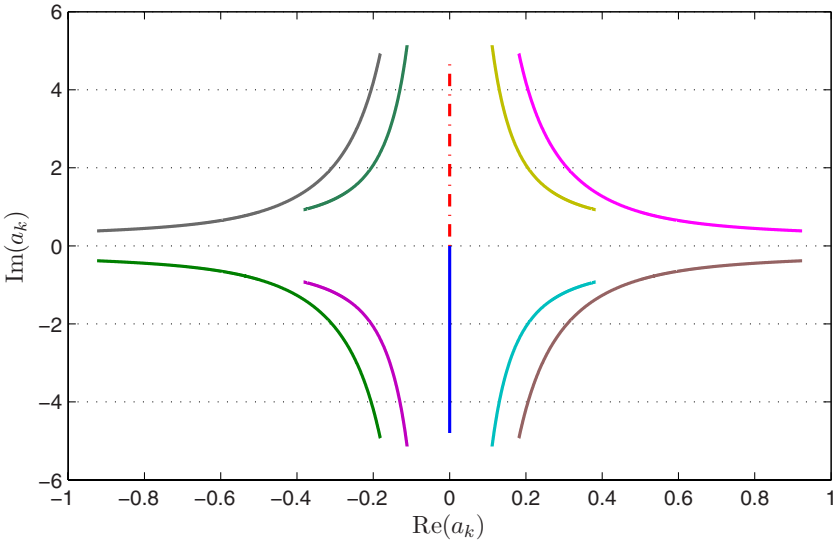

FIG. 5. (Color online) Ten solutions of $\hat{P}(a_k)=0$ for $\alpha=2/5$, and $\gamma=1$, in the imaginary plane, for $0<\omega<5$. All ten solutions are different and do not coincide; namely, for this case there does not exist a critical frequency ω_c since $q=5$ is odd. The origin corresponds to $\omega=0$.

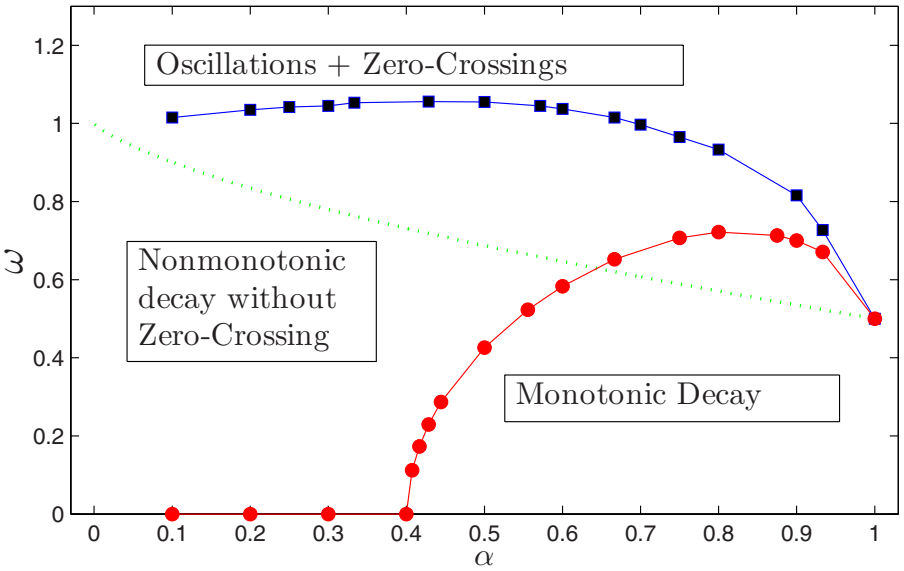

FIG. 6. (Color online) Phase diagram of the fractional oscillator. Phase (a) monotonic decay of the correlation function $C_x(t)$, phase (b) nonmonotonic decay without zero crossing, and phase (c) oscillations with zero crossings. The boundary between (b) and (c) is $\omega_z=\kappa_z(\alpha)$ (solid line + squares); the boundary between (a) and (b) is $\omega_m=\kappa_m(\alpha)$ (solid line + circles). For $\alpha<\alpha_c\simeq 0.402$, the phase of monotonic decay disappears, namely, we do not find overdamped behavior. The dotted curve is the critical line ω_c given by Eq. (59). All the curves are calculated for $\gamma=1$. For $\alpha=1$, $\omega_c=\omega_z=\omega_m=\gamma/2$.

$$\hat{P}(s)=0, \quad \frac{d\hat{P}(s)}{ds}=0. \tag{55}$$

Using Eq. (29) with $\alpha=\frac{p}{q}$ and $\omega=\omega_c$,

$$(s^2+\omega_c^2)^q+(-1)^{q-1}\gamma^q s^p=0 \tag{56}$$

$$2qs(s^2+\omega_c^2)^{q-1}+p(-1)^{q-1}\gamma^q s^{p-1}=0. \tag{57}$$

Solving these Eqs. we find

$$s=\pm\sqrt{\frac{\alpha}{2-\alpha}}\omega_c \tag{58}$$

and ω_c must satisfy

$$\omega_c=\frac{1}{2^{1/(2-\alpha)}}\sqrt{(2-\alpha)\alpha^{\alpha/(2-\alpha)}}\gamma^{1/(2-\alpha)}. \tag{59}$$

Equation (58) and Eq. (59) are only valid for even q or even $(q+p)$ (recall $\alpha=(p/q)$ and (p/q) is irreducible), since for any other case Eqs. (56) and (57) has no solutions. The + sign in Eq. (58) is for the case of even q and odd p and the − sign for odd q and p. To see this, insert the solution Eq. (58) in Eq. (56) and then we must have $(-1)^{q-1}<0$ and hence q even, since (p/q) is irreducible p is odd. Similarly for the − sign in Eq. (58). From this discussion it becomes clear why there are no critical frequency ω_c for $\alpha=(2/5)$ (Fig. 5).

B. Critical points ω_z and ω_m

We divide the phase space to three different regions. (*I*) $0<\omega<\omega_m$ the region where $C_x(t)$ decays monotonically (*II*) $\omega_m<\omega<\omega_z$ the region of nonmonotonic decay while $C_x(t)$ always stays positive (*III*) $\omega_z<\omega$ the region of nonmonotonic decay while part of the time $C_x(t)$ is negative. Similar to Eq. (59) we find from dimensional analysis

$$\omega_z=\kappa_z(\alpha)\gamma^{1/(2-\alpha)} \tag{60}$$

and

$$\omega_m=\kappa_m(\alpha)\gamma^{1/(2-\alpha)} \tag{61}$$

where $\kappa_z(\alpha)$ and $\kappa_m(\alpha)$ depend only on α. By investigating analytical solution Eq. (26) for various α and $\gamma=1$ we obtain functions $\kappa_z(\alpha)$ and $\kappa_m(\alpha)$. The resulting phase diagram is presented in Fig. 6. One can readily see that ω_z, ω_m and ω_c defined by Eq. (59) all coincide only for the normal case $\alpha=1$.

An interesting behavior is observed for $\kappa_m(\alpha)$, as can be seen in Fig. 6 a sort of phase transition occurs around $\alpha\approx 0.4$. We used the general method developed in Sec. III and explored the behavior of $\frac{1}{\omega^2}\frac{dC_x(t)}{dt}$, which in Laplace space is given by

$$\frac{1}{\omega^2}[s\hat{C}_x(s)-1]=-\frac{1}{s^2+\gamma s^\alpha+\omega^2}. \tag{62}$$

For $\alpha\leq 0.4$ we always observed zero crossings for $[dC_x(t)/dt]$ even if we decreased ω to 10^{-7} $(\gamma=1)$, while for $\alpha\geq 0.404$ there were no zero crossings beneath some finite $\omega>0$, as is shown in Fig. 6. So we conclude that there exist a critical α, $\alpha_c\approx 0.402\pm 0.002$, where for $\alpha<\alpha_c$ $C_x(t)$ does not decay monotonically even if the frequency of the binding harmonic field $\omega\to 0$. Note that the phase diagram Fig. 6 also exhibits some expected behaviors: as we increase ω we find a critical line above which the solutions are nonmonotonic and exhibit zero crossing, a line represented by $\kappa_z(\alpha)$.

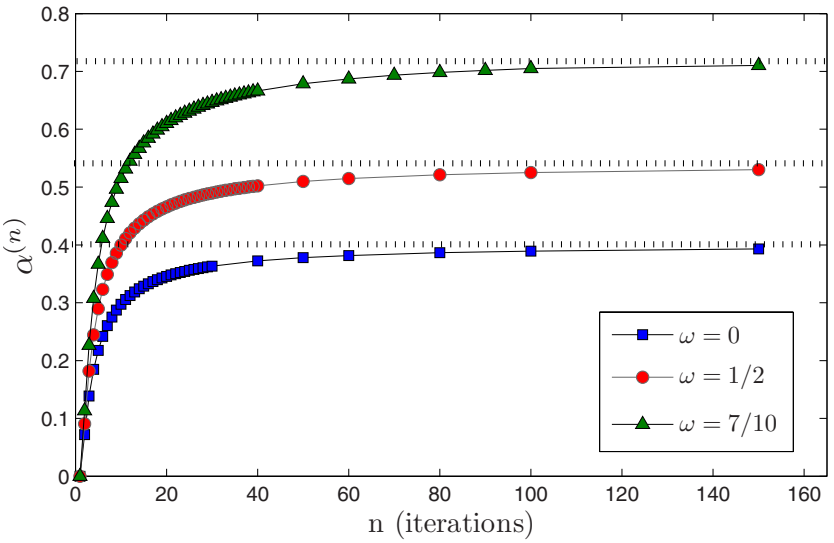

FIG. 7. (Color online) Upper bound $\alpha^{(n)}$ as a function of n, the number of the derivatives, found using the Bernstein method. We consider three different ω (ω=0, 1/2, and 7/10). The dashed lines present the values found numerically in Fig. 6. As n grows, a convergence of the bound is achieved, as is seen for ω=0 as $\alpha^{(n)}$ converges to $\alpha_c \approx 0.402 \pm 0.002$.

To find accurate values of α_c we also used a method based on the Bernstein theorem [38]. According to the theorem, if and only if $f(t)$ is positive then for any integer n

$$0 \leq (-1)^n \frac{d^n \tilde{f}(s)}{ds^n} \quad (s > 0), \tag{63}$$

where $\tilde{f}(s)$ is the Laplace pair of $f(t)$. As in the previous paragraph, in order to check the monotonicity of $C_x(t)$, we will inspect $\frac{1}{\omega^2}\frac{dC_x(t)}{dt}$ for zero crossings, or, speaking in the language of the Bernstein theorem, explore $(-1)^n \frac{d^n \tilde{f}(s)}{ds^n}$, when $-\tilde{f}(s)$ is given by Eq. (62). Using the scaling relation of Eq. (61) we can set γ=1, and so it is easily checked that for n =0 and n=1 $(-1)^n \frac{d^n \tilde{f}(s)}{ds^n} > 0$, for any $0 < \alpha < 1$. But for n=2

$$(-1)^n \frac{d^n \tilde{f}(s)}{ds^n} = \frac{1}{(s^2 + s^\alpha + \omega^2)^3}\{6s^2 + (9\alpha - \alpha^2 - 2)s^\alpha + (\alpha^2 + \alpha)s^{2\alpha-2} - \omega^2[2 + \alpha(\alpha - 1)]s^{\alpha-2}\}, \tag{64}$$

and in the limit $\omega \to 0$ one can easily show that for $\alpha \leq 0.071$ Eq. (64) has negative values. Actually, for α=0.01 it is easily verified [by plotting Eq. (64)] that for any $\omega > 0$ Eq. (64) would have negative values. So for n=2 we have an upper bound for α, $\alpha^{(2)} \approx 0.071$, where for any $\alpha < \alpha^{(2)}$ $\frac{dC_x(t)}{dt}$ crosses the zero line and the relaxation is nonmonotonic. If one wishes to increase the accuracy for such an upper bound one should inspect the behavior of $(-1)^n \frac{d^n \tilde{f}(s)}{ds^n}$ for higher values of n; for any n we define such a bound as $\alpha^{(n)}$. Using MATHEMATICA we can proceed to higher values of n and find the upper bound $\alpha^{(n)}$ for different ω. In Fig. 7 we plotted the upper bounds as a function of n for various ω; we see that as n grows the upper bound $\alpha^{(n)}$ converges to some value <1. The results achieved by this method converge to values very close to the values displayed in Fig. 6; for example, for ω =0 and n=150 $\alpha^{(150)}$=0.394, compared with $\alpha_c \approx 0.402$, obtained by inspection of the exact solution.

C. Cage effect

A physical explanation for this interesting result is based on the cage effect. For small α the friction force induced by the medium is not just slowing down the particle but also causing the particle to develop a rattling motion. To see this, consider Eq. (8) in the limit $\alpha \to 0$,

$$m\ddot{C}_x(t) + m\gamma[C_x(t) - C_x(0)] + m\omega^2 C_x(t) = 0, \tag{65}$$

where from Eq. (6) $C_x(0)$=1. Equation (65) describes harmonic motion and the friction γ in this $\alpha \to 0$ limit yields an elastic harmonic force. In this sense the medium is binding the particle, preventing diffusion but forcing oscillations. In the opposite limit of $\alpha \to 1$,

$$m\ddot{C}_x(t) + m\gamma\dot{C}_x(t) + m\omega^2 x = 0, \tag{66}$$

the usual damped oscillator is found. So from Eq. (65) an oscillating behavior is expected, even when $\omega \to 0$, which can be explained by the rattling motion of a particle in the cage formed by the surrounding particles. This behavior manifests in the nonmonotonic oscillating solution we have found for small α. Our finding that α_c marks a nonsmooth transition between normal friction $\alpha \to 1$ and elastic friction $\alpha \to 0$ is certainly a surprising result.

The existence of a cage effect for small enough α is observed not only for the correlation function but also for other quantities. In the next section we will show the existence of an oscillating mode for the complex susceptibility. Such a mode appears for high enough frequencies and low enough α's. The existence of an oscillating mode coincides with the description of Eq. (65) for the correlation function and emphasizes that such an oscillatory motion is not due to a specific properties of the measured quantity but rather due to the complex interaction of the particle with the medium as described by the friction term.

VI. RESPONSE TO AN EXTERNAL FIELD

In this section we will explore the response of the FLE to an external time-dependent force. The response of a system

to an oscillating time-dependent field naturally leads to the phenomenon of resonances, when the frequency of the external field matches a natural frequency of the system. The response of subdiffusing systems to such a time-dependent field has been the subject of intensive research [39–41]. In particular, the fractional approach to subdiffusion naturally leads to anomalous response functions commonly found in many systems e.g., the Cole-Cole relaxation [28,42,43]. In the next three sections we will explore the response of the FLE with and without the harmonic potential and also investigate the behavior of the imaginary part of the complex susceptibility, i.e., the dielectric loss, for these cases.

Our starting point is Eq. (2) with $F(x,t)=F_0\cos(\Omega t)-m\omega^2 x$; performing an average we obtain

$$\langle \ddot{x}\rangle + \gamma \frac{d^\alpha \langle x\rangle}{dt^\alpha} + \omega^2\langle x\rangle = \frac{F_0}{m}\cos(\Omega t). \tag{67}$$

The solution in the long-time regime is

$$\langle x(t)\rangle \sim \frac{F_0}{m}\int_0^t \cos[\Omega(t-t')]h(t')dt', \tag{68}$$

where $h(t)$ is soon defined. Equation (68) is written as

$$\langle x(t)\rangle = R(\Omega)\cos[\Omega t+\theta(\Omega)], \quad t\to\infty. \tag{69}$$

The response $R(\Omega)$ and the phase shift $\theta(\Omega)$ are obtained by means of the complex susceptibility

$$\chi(\Omega)=\chi'(\Omega)+i\chi''(\Omega)=\hat{h}(-i\Omega), \tag{70}$$

where $\chi'(\Omega)$ and $\chi''(\Omega)$ are the complex and the imaginary parts of the susceptibility, respectively, and $\hat{h}(-i\Omega)=\int_o^\infty e^{i\Omega t}h(t)dt$ [19]. For the response

$$R(\Omega)=|\chi(\Omega)|, \tag{71}$$

and

$$\theta(\Omega)=\arctan\left(-\frac{\chi''(\Omega)}{\chi'(\Omega)}\right) \tag{72}$$

for the phase shift.

A. Unbound particle

For the unbound particle we set $\omega=0$ in Eq. (67) and using Eq. (4) we obtain for $\chi(\Omega)$

$$\chi(\Omega)=\hat{h}(-i\Omega)=\frac{1}{\gamma(-i\Omega)^\alpha-\Omega^2}. \tag{73}$$

By the use of Eq. (71) we can explicitly obtain now the behavior of $R(\Omega)$ for any $0<\alpha<1$. For the normal diffusion case when $\alpha=1$, the response $R(\Omega)$ is a decaying function of Ω and no resonance is observed, but the picture is quite different for $0<\alpha<1$. In this subdiffusive part the response $R(\Omega)$ is not always a monotonically decaying function and could obtain a maximum, i.e., a resonance, even for such a free motion. As is seen in Fig. 8, for small enough α, $R(\Omega)$ has a resonance; we will show that the existence of the resonance does not depend on any other parameter but α.

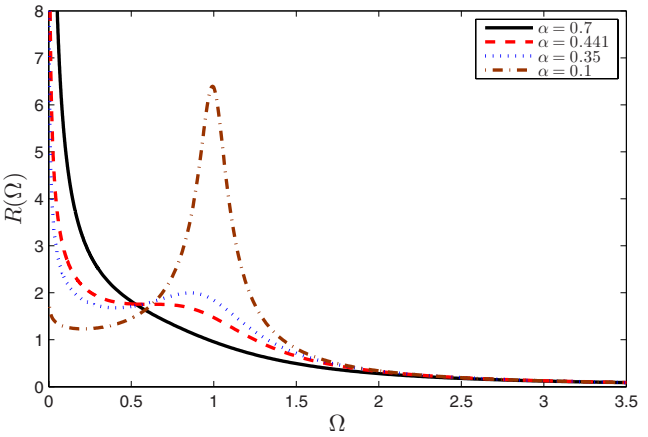

FIG. 8. (Color online) Response of FLE to an oscillating field for a free particle and different α's. For $\alpha<\alpha_R$ a resonance is observed. All the curves are plotted with $\gamma=1$.

Writing down the response $R(\Omega)$ explicitly, we have

$$R(\Omega)=\frac{1}{\sqrt{\Omega^4+\gamma^2\Omega^{2\alpha}-2\gamma\Omega^{2+\alpha}\cos(\pi\alpha/2)}}. \tag{74}$$

We are looking for the solutions of $dR(\Omega)/d\Omega=0$, and hence

$$4\Omega_R^3+2\alpha\gamma^2\Omega_R^{2\alpha-1}-2(\alpha+2)\gamma\Omega_R^{\alpha+1}\cos\left(\frac{\pi\alpha}{2}\right)=0, \tag{75}$$

so the solution is

$$\frac{\gamma}{\Omega_R^{2-\alpha}}=\frac{1}{2\alpha}\left[(\alpha+2)\cos\left(\frac{\pi\alpha}{2}\right) \pm \sqrt{(\alpha+2)^2\cos^2\left(\frac{\pi\alpha}{2}\right)-8\alpha}\right], \tag{76}$$

and Ω_R is the frequency for which the resonance is found. When the discriminant on the right of Eq. (76) is greater than zero there will be a resonance. The discriminant has no dependence on γ, and is always positive for $\alpha\le\alpha_R=0.441\,021\ldots$, which satisfies the relation

$$(\alpha_R+2)^2\cos^2\left(\frac{\pi\alpha_R}{2}\right)-8\alpha_R=0. \tag{77}$$

So no resonance is found for $\alpha>\alpha_R$, and for $\alpha<\alpha_R$ there is always an $\Omega_R>0$ for which the response will exhibit a resonance. This result of a resonance for a free particle FLE is highly unexpected, but agrees well with our description of the friction force for small α as an elastic force due to the cage effect.

B. Harmonically bound particle

Now we treat the response function of the FLE with a harmonic field, i.e., that of a fractional oscillator. Starting with Eq. (67), we set the initial conditions $x_0=v_0=0$ and in the long-time limit $t\to\infty$ we obtain again $\langle x\rangle=R(\Omega)\cos[\Omega t+\theta(\Omega)]$ where $R(\Omega)$ and $\theta(\Omega)$ are defined by Eqs. (71) and

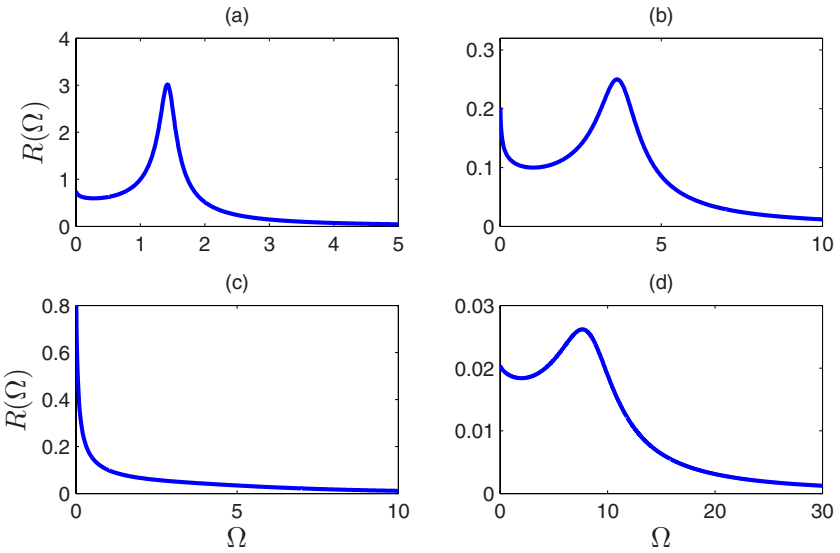

FIG. 9. (Color online) Response of FLE to an oscillating field for a harmonically bound particle and different α. (a) $\alpha=0.2$, $\omega=1$, and $\gamma=1$. (b) $\alpha=0.2$, $\omega=1$, and $\gamma=10$. (c) $\alpha=0.7$, $\omega=1$, and $\gamma=10$. (d) $\alpha=0.7$, $\omega=7$, and $\gamma=10$.

(72). The complex susceptibility for this case is obtained as

$$\chi(\Omega) = \frac{1}{(\omega^2 - \Omega^2) + \gamma(-i\Omega)^\alpha}. \tag{78}$$

Equation (78) was already obtained [46–48] for the fractional Klein-Kramers equation [24] in the high-damping limit and is called a generalized Rocard equation [49,50]. For $\alpha=1$ we find the complex susceptibility of a normal damped oscillator.

We are interested in the resonance points for the response to the applied field, i.e., points of maximum of $R(\Omega)$, which generally depend on Ω, γ, and ω (see Fig. 9). For the normal oscillator there is a resonance if the condition $\omega \geq \frac{1}{\sqrt{2}}\gamma$ is satisfied. If this condition is not satisfied, $R(\Omega)$ is a monotonically decreasing function of Ω. From Eqs. (71) and (78)

$$R(\Omega) = \frac{1}{\sqrt{(\omega^2 - \Omega^2)^2 + \gamma^2\Omega^{2\alpha} + 2(\omega^2 - \Omega^2)\gamma\Omega^\alpha \cos(\pi\alpha/2)}}, \tag{79}$$

and using $dR(\Omega)/d\Omega=0$ we find

$$2\alpha\left(\frac{\gamma}{\Omega_R^{2-\alpha}}\right)^2 + \left[2\alpha\left(\frac{\omega^2}{\Omega_R^2} - 1\right) - 4\right] \times \cos\left(\frac{\pi\alpha}{2}\right)\frac{\gamma}{\Omega_R^{2-\alpha}} - 4\left(\frac{\omega^2}{\Omega_R^2} - 1\right) = 0. \tag{80}$$

The exploration of Eq. (80) (see Appendix B) leads to two findings which are presented in Fig. 10. The first one is the existence of the same critical α_R given by Eq. (77) for the response of the FLE with a harmonic potential, i.e., for any $\alpha<\alpha_R$ there always exists a specific Ω_R (which depends on γ and ω) for which the system is in resonance. The second finding is that above α_R we have a well-defined boundary between a phase for which the resonance exists—a resonance phase— and a phase where there is no resonance—a no-resonance phase (see Fig. 10). For $\alpha<\alpha_R$ the no-resonance phase does not exists. The boundary is given by the following relation:

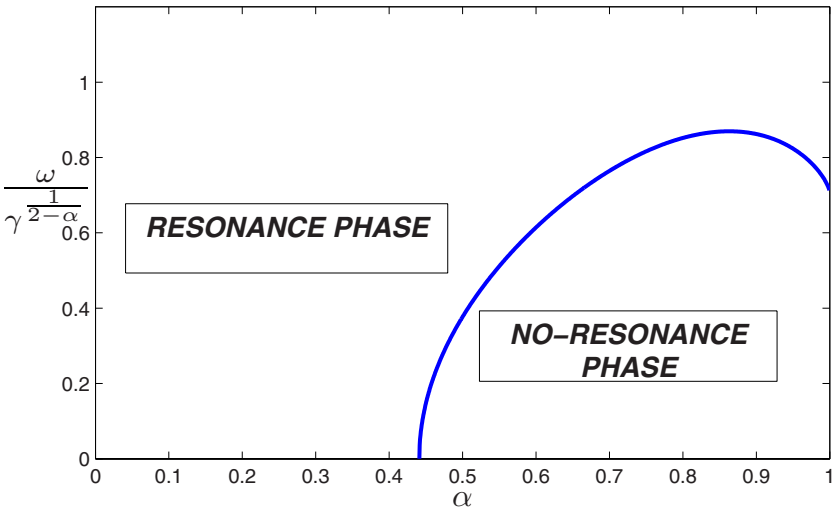

FIG. 10. (Color online) Phase diagram of the response of the system with a harmonic field to an oscillating time-dependent force field. Two simple behaviors are found: either a resonance exists (resonance phase) or not (no-resonance phase). For $\alpha<\alpha_R$ $=0.441\ldots$ a resonance exists for any binding harmonic field and any friction γ.

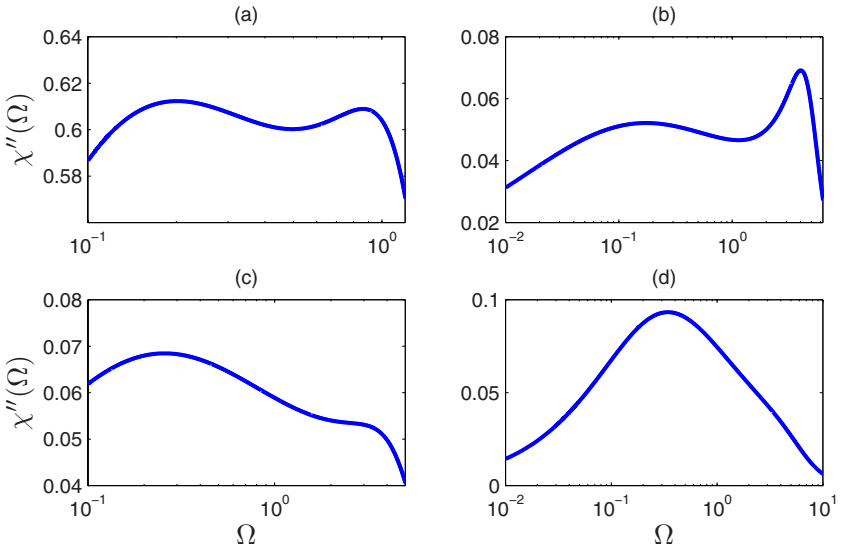

FIG. 11. (Color online) Imaginary part of the complex susceptibility for various α. A double-peak phenomenon is observed. (a) $\alpha=0.66$, $\gamma=1.8$, and $\omega=0.7$. (b) $\alpha=0.5$, $\gamma=10$, and $\omega=2$. (c) $\alpha=0.63$, $\gamma=10$, and $\omega=2$. (d) $\alpha=0.8$, $\gamma=10$, and $\omega=2$.

$$\frac{\omega}{\gamma^{1/(2-\alpha)}} = g(\alpha), \tag{81}$$

and the phase diagram is presented in Fig. 10. The function $g(\alpha)$ is found analytically (see Appendix B),

$$g(\alpha) = c(\alpha)^{-1/(2-\alpha)} \sqrt{\frac{c(\alpha)^2 - c(\alpha)\cos(\pi\alpha/2)\left(1+\frac{2}{\alpha}\right) + 2/\alpha}{2/\alpha - c(\alpha)\cos(\pi\alpha/2)}}, \tag{82}$$

where $c(\alpha)$ is given by Eq. (B13). As is seen from Fig. 10 for $\omega/\gamma^{1/(2-\alpha)} > g(\alpha)$ a resonance phase is obtained, and the no-resonance phase for $\omega/\gamma^{1/(2-\alpha)} < g(\alpha)$. In the limit of $\alpha \to 1$ the boundary goes to the expected value for a damped oscillator, $1/\sqrt{2}$. Near the critical point α_R, the $g(\alpha)$ drops to zero as a power law with exponent ½,

$$g(\alpha) \propto (\alpha - \alpha_R)^{1/2}, \quad \alpha \to \alpha_R. \tag{83}$$

The existence of the same critical α_R for a free and a harmonically bound particle is easily understood from the phase diagram in Fig. 10. Choosing the straight line $\omega=0$, which represents the free particle, and going along this line, when starting at the resonance phase we will cross to the no-resonance phase exactly for $\alpha=\alpha_R$. Generally speaking, the same critical α_R will be obtained for any kind of external force because it is determined by the internal properties of the surrounding medium represented by the friction part in the FLE. The phase diagram in Fig. 10 has much in common with the phase diagram in Fig. 6, which is quite reasonable because of the strong connection between nonmonotonic decay of the correlation $C_x(t)$ and existence of a resonance. The presence of a resonance for small enough α emphasizes the previously obtained result of nonexistence of the overdamped limit for such α. Those properties are due to the same cage effect that we already discussed.

C. Complex susceptibility

Equation (78) for the complex susceptibility can be written in the following form:

$$\chi(\Omega) = \chi'(\Omega) + i\chi''(\Omega) = \frac{(\omega^2 - \Omega^2) + \gamma\Omega^\alpha \cos(\pi\alpha/2)}{(\omega^2 - \Omega^2)^2 + \gamma^2\Omega^{2\alpha} + 2\gamma(\omega^2 - \Omega^2)\Omega^\alpha \cos(\pi\alpha/2)} + i\frac{\gamma\Omega^\alpha \sin(\pi\alpha/2)}{(\omega^2 - \Omega^2)^2 + \gamma^2\Omega^{2\alpha} + 2\gamma(\omega^2 - \Omega^2)\Omega^\alpha \cos(\pi\alpha/2)}. \tag{84}$$

The real and the imaginary parts of the susceptibility are experimentally measured quantities for many systems, and so it is interesting to explore their behavior for the FLE. In this section we will explore the behavior of the imaginary part $\chi''(\Omega)$, which is also called the loss. From Fig. 11, we observe interesting behavior of $\chi''(\Omega)$ for different α's; not only is one peak present as is expected for the normal oscillator, but we observe a double-peak phenomenon for some α's. The double-peak phenomenon of the loss for supercooled liquids and protein solutions is a well-known phenomenon [51–53] and usually treated by means of mode-coupling theory [52]. We define two phases for the behavior of $\chi''(\Omega)$ and in the following find the phase diagram for $\chi''(\Omega)$. The first phase is the phase where $\chi''(\Omega)$ has only one peak, the one-peak phase, and a double-peak phase, where the double-peak phenomenon is observed.

In Appendix C we explore $d\chi''(\Omega)/d\Omega$ and search for the boundaries between the one-peak and double-peak phases. The result is presented in Fig. 12. The boundaries between the phases are given by analytical functions $\tilde{g}_1(\alpha)$ and $\tilde{g}_2(\alpha)$ which are dependent only on α. Two critical α are found for such a phase diagram, the first one $\alpha_{\chi_1}=0.527\ldots$ for which the boundary $\tilde{g}_1(\alpha)$ drops to zero, and a second one $\alpha_{\chi_2}=0.707\ldots$ for which $\tilde{g}_1(\alpha)$ and $\tilde{g}_2(\alpha)$ coincide (see Fig. 11). We also must note that near α_{χ_1} $\tilde{g}_1(\alpha)$ behaves as $\tilde{g}_1(\alpha) \propto (\alpha - \alpha_{\chi 1})^{1/2}$, a behavior that was also observed for $g(\alpha)$ and $\kappa_m(\alpha)$ near the corresponding critical points.

The double-peak phenomenon in our case is explained in the same sense as the existence of resonance for small enough α and the disappearance of the monotonic decay phase for the correlation function were explained. The reason

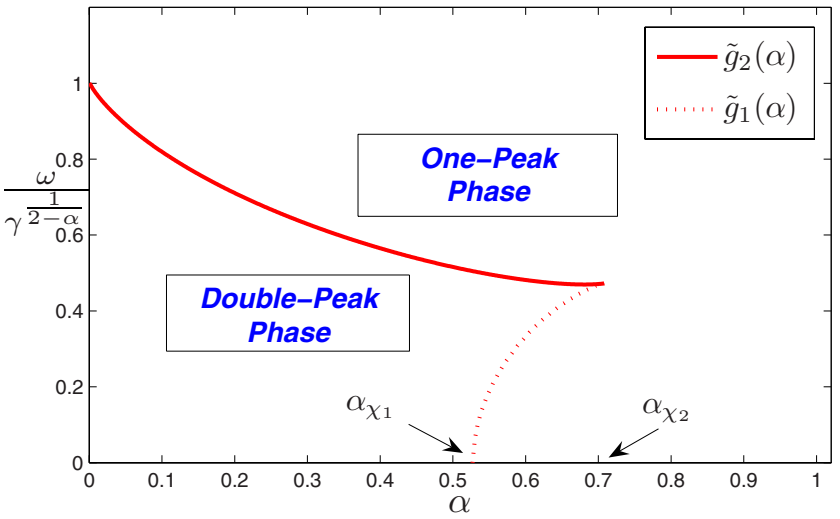

FIG. 12. (Color online) Phase diagram of the imaginary part of the complex susceptibility. Two phases are found, a phase with one maximum for $\chi''(\Omega)$ (one-peak phase) and a phase with two maxima (double-peak phase). For $\alpha > \alpha_{\chi_2} = 0.707\ldots$ only one phase is present.

is the same: the friction becomes more of an elastic force for such small-α embedding oscillations in the system. Such a claim is emphasized by the Cole-Cole plots of the complex susceptibility, presented in Fig. 13. For $\alpha=0.8$ the behavior is very much as for a normal damped oscillator, a Debye model [19], for small enough $\omega/\gamma^{1/(2-\alpha)}$ (large friction) as in Fig. 13(c), i.e., a monotonic behavior for the relaxation; and a Van Vleck–Weisskopf–Fröhlich type of behavior [19] for a large value of $\omega/\gamma^{1/(2-\alpha)}$ (small friction) as in Fig. 13(d), i.e., an oscillating behavior of the relaxation. These two prototypes of the normal complex susceptibility correspond to the presence of a single characteristic frequency in the system, or a single time scale if we are concerned with correlations. For small α, such as $\alpha=0.1$ in Fig. 13(a), we see a coexistence of these two types of normal susceptibility. The right side of Fig. 13(a) corresponds to a Debye type, a monotonically decaying process, and the left side to a Van Vleck–Weisskopf–Fröhlich type, which shows highly oscillating behavior even in the case when γ and ω are the same as for Fig. 13(c). Effectively, for small α we have two characteristic frequencies in the system; the lower is responsible for the monotonic decay and the higher frequency is an oscillating process. For intermediate α we have some mixed behavior—Fig. 13(b). This oscillating behavior that is seen in Fig. 13(a) is the manifestation of the cage effect which we already explained as the rattling motion of the surrounding particles and is present in the FLE due to the friction force.

VII. SUMMARY

The fractional Langevin equation with power law memory kernel and $0<\alpha<1$ is a stochastic framework describing anomalous subdiffusive behavior. This equation may be expressed in terms of fractional derivatives and so provides an example of a physical phenomenon where noninteger calculus plays a central role. The solution of a fractional-differential equation describing the correlation function was presented in terms of roots of regular polynomials. It was shown that for $\alpha \neq 1$ there is no unique way to define an overdamped or underdamped motion. Three definitions were proposed for the frequency of transition, i.e., ω_c, ω_m, and ω_z. We observed the existence of a phase transition for a critical $\alpha=\alpha_c \approx 0.402$, where for $\alpha<\alpha_c$ $C_x(t)$ does not decay monotonically for any $\omega>0$. Physically it is explained using the

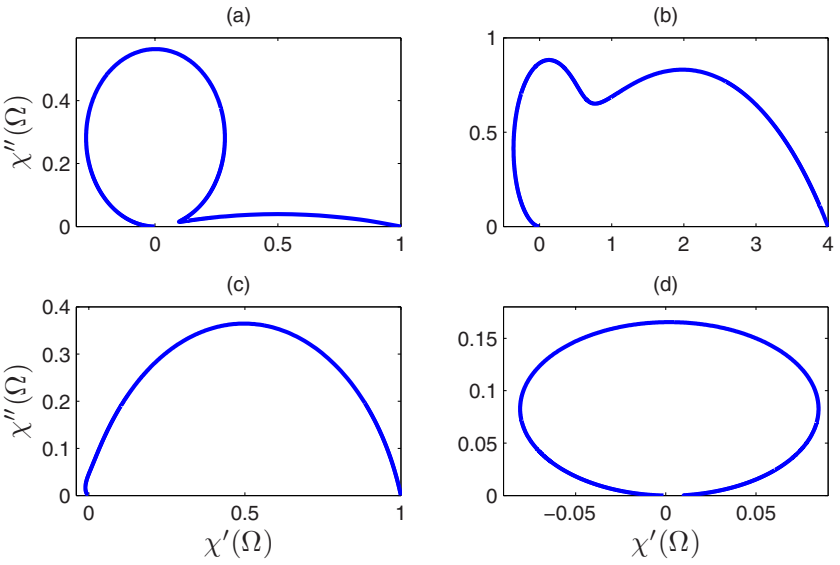

FIG. 13. (Color online) Cole-Cole plots of the complex susceptibility $\chi''(\Omega)$ as a function of $\chi'(\Omega)$. (a) $\alpha=0.1$, $\gamma=10$, and $\omega=1$. (b) $\alpha=0.5$, $\gamma=10$, and $\omega=0.5$. (c) $\alpha=0.8$, $\gamma=10$, and $\omega=1$. (d) $\alpha=0.8$, ,$\gamma=1$ and $\omega=10$. (c) and (d) show two typical normal behaviors; for small α (a) and (b) show a behavior that is a mixture of the two normal typical behaviors.

cage effect: a rattling motion of the particle in the cage formed by the surrounding particles. The response to a time-dependent field in terms of the complex susceptibility $\chi(\Omega)$ was also calculated and similar critical α's were found. Particularly for $\alpha<\alpha_R=0.441\ldots$, the system will always be in resonance with the external field for a particular Ω and any γ and ω, even in the case of a free particle ($\omega=0$). For the loss, the imaginary part of the complex susceptibility, $\chi''(\Omega)$, two phases were defined: (i) the one-peak phase where the complex susceptibility obtains only one maximum as in a regular case, and (ii) the double-peak phase, where the complex susceptibility obtains two maxima. A phase diagram was presented. Two critical exponents $\alpha_{\chi_1}=0.527\ldots$ and $\alpha_{\chi_2}=0.707\ldots$ were found for $\chi''(\Omega)$, exponents which define the boundaries of the phase diagram. In conclusion, critical exponents like α_c, α_R, α_{χ_1}, and α_{χ_2} mark sharp transitions in the behaviors of systems with fractional dynamics. Thus, these critical exponents are clearly important and general in the description of anomalous kinetics.

ACKNOWLEDGMENT

This work was supported by the Israel Science Foundation.

APPENDIX A: THE SOLUTION FOR NONDISTINCT ZEROS OF $\hat{P}(s)$

In this appendix we derive the solution of Eq. (12) for the case when two zeros of $\hat{P}(s)$ coincide. This means that $\hat{P}(s)$ has $2q-2$ distinct zeros of order 1 and one zero of order 2. Namely, at the critical point ω_c only two a_k coincide and we present here a method of solution for $\omega=\omega_c$.

Starting with Eq. (12), we write the partial fraction expansion in the following way:

$$\frac{1}{\hat{P}(s)}=\sum_{k=1}^{2q-1}\frac{A_k}{s-a_k}+\frac{\tilde{A}}{(s-a_{2q-1})^2}, \tag{A1}$$

where a_k are the zeros of $\hat{P}(s)$ and we assign a_{2q-1} to be the zero of the second order. A_k and $\tilde{A}$ are given by

$$A_k=\frac{1}{\left.\frac{d\hat{P}(s)}{ds}\right|_{s=a_k}}, \quad 1\le k<2q-1, \tag{A2}$$

$$A_{2q-1}=-\sum_{k=1}^{2q-2}A_k, \tag{A3}$$

and

$$\tilde{A}=\frac{1}{\left.\frac{d}{ds}\frac{\hat{P}(s)}{s-a_{2q-1}}\right|_{s=a_{2q-1}}}. \tag{A4}$$

Using the relation [21]

$$\sum_{k=1}^{2q-1}a_k^m A_k+ma_k^{m-1}\tilde{A}=0, \quad m=0,1,\ldots,2q-2, \tag{A5}$$

one finds that

$$\frac{s^m}{\hat{P}(s)}=\sum_{k=1}^{2q-1}\frac{A_k a_k^m}{s-a_k}+\frac{ma_{2q-1}^{m-1}\tilde{A}}{s-a_{2q-1}}+\frac{a_{2q-1}^m\tilde{A}}{(s-a_{2q-1})^2}, \quad m=0,1,\ldots,2q-1. \tag{A6}$$

Hence using Eqs. (12), (18), and (A6)

$$\hat{C}_x(s)=\sum_{m=0}^{2q-1}\sum_{j=0}^{q-1}\left(\sum_{k=1}^{2q-1}\frac{a_k^m A_k\tilde{B}_{mj}}{s-a_k}s^{-j/q}+\frac{ma_{2q-1}^{m-1}\tilde{A}\tilde{B}_{mj}}{s-a_{2q-1}}s^{-j/q}+\frac{a_{2q-1}^m\tilde{A}\tilde{B}_{mj}}{(s-a_{2q-1})^2}s^{-j/q}\right), \tag{A7}$$

and it is only left to perform an inverse Laplace transform of $1/[s^{j/q}(s-a_{2q-1})^2]$, using the convolution theorem

$$\frac{1}{s^{j/q}(s-a_{2q-1})^2}\multimap \frac{te^{a_{2q-1}t}}{\Gamma\left(\frac{j}{q}\right)a_{2q-1}^{j/q}}\gamma\left(\frac{j}{q},a_{2q-1}t\right)-\frac{e^{a_{2q-1}t}}{\Gamma\left(\frac{j}{q}\right)a_{2q-1}^{j/q+1}}\gamma\left(\frac{j}{q}+1,a_{2q-1}t\right) \tag{A8}$$

or the Mittag-Leffler function

$$\frac{1}{s^{j/q}(s-a_{2q-1})^2}\multimap t^{j/q+1}E_{1,1+j/q}(a_{2q-1}t)-\frac{j}{q}t^{j/q+1}E_{1,2+j/q}(a_{2q-1}t). \tag{A9}$$

Finally, using Eqs. (21), (A7), and (A8),

$$C_x(t)=\sum_{m=0}^{2q-1}\sum_{j=0}^{q-1}\frac{\tilde{B}_{mj}}{\Gamma(j/q)}\left\{\sum_{k=1}^{2q-1}a_k^{m-j/q}A_k e^{a_k t}\gamma\left(\frac{j}{q},a_k t\right)+a_{2q-1}^{m-j/q}\tilde{A}e^{a_{2q-1}t}\left[(t+ma_{2q-1}^{-1})\gamma\left(\frac{j}{q},a_{2q-1}t\right)-a_{2q-1}^{-1}\gamma\left(\frac{j}{q}+1,a_{2q-1}t\right)\right]\right\}, \tag{A10}$$

or using Eq. (A9)

$$C_x(t)=\sum_{m=0}^{2q-1}\sum_{j=0}^{q-1}\tilde{B}_{mj}t^{j/q}\left[\sum_{k=1}^{2q-1}a_k^m A_k E_{1,1+j/q}(a_k t)+a_{2q-1}^m\tilde{A}\times\left((t+ma_{2q-1}^{-1})E_{1,1+j/q}(a_{2q-1}t)-\frac{j}{q}tE_{1,2+j/q}(a_{2q-1}t)\right)\right]. \tag{A11}$$

A final remark: one can show that for our case of integer $q>p>0$, third- and higher-order zeros of $\hat{P}(s)$ do not exist.

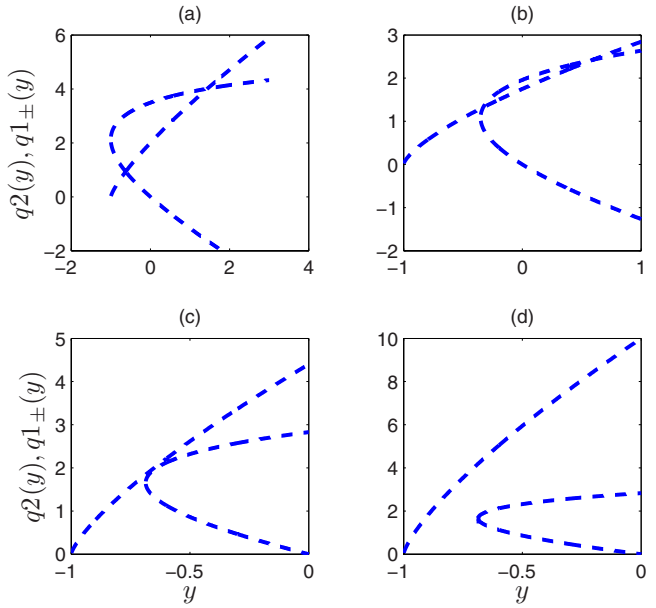

FIG. 14. (Color online) Four scenarios for $q_{1\pm}(y)$ and $q_2(y)$ crossings. Existence of a crossing corresponds to the resonance phase and no crossings correspond to the no-resonance phase. (a) $\alpha=0.441$, $\gamma=2$, and $\omega=1$; for this case there will always be two crossings, $\alpha<\alpha_R$. (b) $\alpha=0.6$, $\gamma=1.75$, and $\omega=1$; this panel corresponds to a resonance phase. (c) $\alpha=0.5$, $\gamma=4.4$, and $\omega=1$, this panel describes a situation on the boundary between resonance and no-resonance phases. (d) $\alpha=0.5$, $\gamma=10$, and $\omega=1$, a no-resonance phase.

APPENDIX B: EXPLORATION OF EQ. (80)

In this appendix we prove the existence of α_R for a FLE with a harmonic force and derive the equation for $g(\alpha)$ given by Eq. (82). Solving Eq. (80), one gets for $\gamma/\Omega_R^{2-\alpha}$

$$\frac{\gamma}{\Omega_R^{2-\alpha}} = \frac{1}{2\alpha}\left[[2-\alpha y]\cos\left(\frac{\pi\alpha}{2}\right)\right] \pm \frac{1}{2\alpha}\sqrt{\left[[2-\alpha y]^2\cos\left(\frac{\pi\alpha}{2}\right)\right]^2 + 8\alpha y} = q_{1\pm}(y), \tag{B1}$$

and $y=(\omega^2/\Omega_R^2-1)>-1$. Writing the left-hand side of Eq. (B1) in terms of y,

$$\frac{\gamma}{\Omega_R^{2-\alpha}} = \frac{\gamma}{\omega^{2-\alpha}}(y+1)^{1-\alpha/2} = q_2(y). \tag{B2}$$

We see that for the extremal points of $R(\Omega)$ the functions $q_{1\pm}(y)$ and $q_2(y)$ cross each other (see Fig. 14). While $q_2(y)$ is a monotonically increasing function starting from zero for $y=-1$ and growing as $y^{1-\alpha/2}$ for large y, $q_{1\pm}(y)$ constructs two branches where $q_{1+}(y)$ is the upper branch and $q_{1-}(y)$ is the lower branch and for some point y_α

$$q_{1-}(y_\alpha) = q_{1+}(y_\alpha) = \frac{(2-\alpha y_\alpha)\cos(\pi\alpha/2)}{2\alpha}. \tag{B3}$$

If $y_\alpha<-1$ then $q_2(y)$ crosses $q_{1\pm}(y)$ no matter what the parameters γ, ω, and α are, because in that case for $y=-1$ $q_{1\pm}(y)>0$ and $q_2(y)=0$ and a resonance is always obtained. The point y_α is derived from Eq. (B1) and determined by the following relation:

$$(2-\alpha y_\alpha)^2\cos^2\left(\frac{\pi\alpha}{2}\right) + 8\alpha y_\alpha = 0. \tag{B4}$$

Solving Eq. (B4) in terms of y_α, one finds

$$y_\alpha = -\frac{2}{\alpha\cos^2(\pi\alpha/2)}\left[1-\sin\left(\frac{\pi\alpha}{2}\right)\right]^2, \tag{B5}$$

where we took the $-$ sign because $y>-1$. For $0<\alpha<1$ Eq. (B5) is an increasing function of α and so we have a critical α, α_R, for $y_\alpha=-1$. Equation (B4) with $y_\alpha=-1$ is exactly Eq. (77), which defines the equation for α_R, and so we have shown the existence of α_R for the harmonically bound particle.

We now argue that the boundary between the resonance phase and no-resonance phase is given by the following relation:

$$\frac{\omega}{\gamma^{1/2-\alpha}} = g(\alpha), \tag{B6}$$

where $g(\alpha)$ is dependent only on α and equals zero for $\alpha\leq\alpha_R$. One readily sees from Eq. (B1) that the large-y behavior of $q_{1\pm}(y)$ is proportional to $\pm\sqrt{y}$, where $q_2(y)$ behaves like $y^{1-\alpha/2}$ for large y [Eq. (B2)]; also we note that $\frac{dq_{1\pm}(y)}{dy}$ and $\frac{dq_2(y)}{dy}$ are monotonically decaying functions of y. As a result we have four options for the scenario of $q_2(y)$ crossing $q_{1\pm}(y)$ (see also Fig. 14): (i) $q_2(y_1)=q_{1-}(y1)$ and $q_2(y_2)=q_{1+}(y2)$ for $y1<y2$; (ii) $q_2(y1)=q_{1+}(y1)$ and $q_2(y2)=q_{1+}(y2)$ for $y1<y2$; (iii) $q_2(y)=q_{1+}(y)$ for a single y; and (iv) $q_2(y)\neq q_{1+}(y)$ and $q_2(y)\neq q_{1-}(y)$ for any y.

When there are two crossings then the one with the larger y corresponds to the minimum and the smaller y corresponds to the maximum and belongs to the resonance phase. When there are no crossings then we are in the no-resonance phase. The scenario (iii) corresponds exactly to the boundary between the two phases. In order to find the boundary, two conditions must be satisfied:

$$q_2(y1) = q_{1+}(y1) \tag{B7}$$

and

$$\frac{dq_2(y)}{dy}|_{y=y1} = \frac{dq_{1+}(y)}{dy}|_{y=y1}, \tag{B8}$$

as illustrated in Fig. 14(c). Starting from Eq. (B7) we compare the left-hand side to some constant c and using Eq. (B2) we find

$$y = c^{2/(2-\alpha)}\left(\frac{\omega}{\gamma^{1/(2-\alpha)}}\right)^2 - 1. \tag{B9}$$

Comparing the right-hand side of Eq. (B7) to the same c and using Eq. (B9) we arrive at the relation

$$\left(\frac{\omega}{\gamma^{1/(2-\alpha)}}\right)^2 = \frac{c^2 - c\,\cos(\pi\alpha/2)(1+2/\alpha)+2/\alpha}{2/\alpha - c\,\cos(\pi\alpha/2)} c^{-2/(2-\alpha)}. \tag{B10}$$

Next, performing the derivation in Eq. (B8) and using Eq. (B9) we find

$$\left(\frac{\omega}{\gamma^{1/(2-\alpha)}}\right)^2 = \frac{(2-\alpha)c\{2c-[1+(2/\alpha)\cos(\pi\alpha/2)]\}}{4/\alpha - 4c\,\cos(\pi\alpha/2)+\alpha c\,\cos(\pi\alpha/2)} c^{-2/(2-\alpha)}. \tag{B11}$$

Comparison of Eqs. (B11) and (B10) supplies an equation for c:

$$\alpha^3\cos\left(\frac{\pi\alpha}{2}\right)c^3 + [2\alpha - 5\alpha^2 - \alpha(2+\alpha)\cos(\pi\alpha)]c^2 + 12\alpha\cos\left(\frac{\pi\alpha}{2}\right)c - 8 = 0. \tag{B12}$$

Equation (B12) has three different solutions where only one is real for $0<\alpha<1$. We will call it $c(\alpha)$ and

$$\begin{aligned} c(\alpha) = \frac{1}{3\alpha^3}\Bigg\{ & \sec\left(\frac{\pi\alpha}{2}\right)\Bigg[-2\alpha+5\alpha^2+2\alpha\cos(\pi\alpha)+\alpha^2\cos(\pi\alpha) - \Bigg[2^{5/3}\alpha^2\sin^2\left(\frac{\pi\alpha}{2}\right)[-4+20\alpha-7\alpha^2+(2+\alpha)^2\cos(\pi\alpha)] \\ & -80\alpha^3+312\alpha^4-384\alpha^5+152\alpha^6-3\alpha^3(-40+132\alpha-126\alpha^2+43\alpha^3)\cos(\pi\alpha)-48\alpha^3\cos(2\pi\alpha)+72\alpha^4\cos(2\pi\alpha) \\ & -24\alpha^6\cos(2\pi\alpha)+8\alpha^3\cos(3\pi\alpha)+12\alpha^4\cos(3\pi\alpha)+6\alpha^5\cos(3\pi\alpha) \\ & +\alpha^6\cos(3\pi\alpha)24\sqrt{6}\sqrt{-\alpha^9\cos^2\left(\frac{\pi\alpha}{2}\right)\left[32-204\alpha+204\alpha^2-59\alpha^3+(2+\alpha)^2(-8+5\alpha)\cos(\pi\alpha)\sin^4\left(\frac{\pi\alpha}{2}\right)\right]} \\ & +\frac{1}{2^{1/3}}\Bigg(\Bigg\{-80\alpha^3+312\alpha^4-384\alpha^5+152\alpha^6-3\alpha^3(-40+132\alpha-126\alpha^2+43\alpha^3)\cos(\pi\alpha)-48\alpha^3\cos(2\pi\alpha) \\ & +72\alpha^4\cos(2\pi\alpha)-24\alpha^6\cos(2\pi\alpha)+8\alpha^3\cos(3\pi\alpha)+12\alpha^4\cos(3\pi\alpha)+6\alpha^5\cos(3\pi\alpha) \\ & +\alpha^6\cos(3\pi\alpha)24\sqrt{6}\sqrt{-\alpha^9\cos^2\left(\frac{\pi\alpha}{2}\right)\left[32-204\alpha+204\alpha^2-59\alpha^3+(2+\alpha)^2(-8+5\alpha)\cos(\pi\alpha)\sin^4\left(\frac{\pi\alpha}{2}\right)\right]}\Bigg\}^{1/3}\Bigg)\Bigg]. \end{aligned} \tag{B13}$$

We thus justified the use of Eq. (B6) and $g(\alpha)$ is given by Eq. (82).

APPENDIX C: EXPLORATION OF $d\chi''(\Omega)/d\Omega$

We start with the exploration of $d\chi''(\Omega)/d\Omega$, where $\chi''(\Omega)$ is given by Eq. (84),

$$\frac{d\chi''(\Omega)}{d\Omega} = \frac{\gamma\Omega^{\alpha+3}\sin(\pi\alpha/2)}{[(\omega^2-\Omega^2)^2+\gamma^2\Omega^{2\alpha}+2\gamma(\omega^2-\Omega^2)\Omega^\alpha\cos(\pi\alpha/2)]^2}\Bigg(\alpha\left[\left(\frac{w_z^2}{\Omega^2}-1\right)^2+\left(\frac{\gamma}{\Omega^{2-\alpha}}\right)^2+2\left(\frac{\omega^2}{\Omega^2}-1\right)\left(\frac{\gamma}{\Omega^{2-\alpha}}\right)\cos\left(\frac{\pi\alpha}{2}\right)\right] - \left\{-4\left(\frac{\omega^2}{\Omega^2}-1\right)+2\alpha\left(\frac{\gamma}{\Omega^{2-\alpha}}\right)^2+2\left[\alpha\left(\frac{\omega^2}{\Omega^2}-1\right)-2\right]\left(\frac{\gamma}{\Omega^{2-\alpha}}\right)\cos\left(\frac{\pi\alpha}{2}\right)\right\}\Bigg), \tag{C1}$$

and we easily see that in order that $\frac{d\chi''(\Omega)}{d\Omega}=0$ the following condition must be satisfied:

$$\alpha\left(\frac{\gamma}{\Omega^{2-\alpha}}\right)^2 - 4\left(\frac{\gamma}{\Omega^{2-\alpha}}\right)\cos\left(\frac{\pi\alpha}{2}\right) - (4y+\alpha y^2) = 0, \tag{C2}$$

where $y=(\frac{\omega^2}{\Omega^2}-1)>-1$. The left-hand side of Eq. (C2) is a second-order polynomial in terms of $\frac{\gamma}{\Omega^{2-\alpha}}$, which is easily solved:

$$\left(\frac{\gamma}{\Omega^{2-\alpha}}\right) = \frac{4\cos(\pi\alpha/2)}{2\alpha} \pm \frac{1}{2\alpha}\sqrt{16\cos^2\left(\frac{\pi\alpha}{2}\right)+4\alpha(4y+\alpha y^2)}. \tag{C3}$$

The right-hand side of Eq. (C3) we will call $\tilde{q}_{1\pm}(y)$ and the left-hand side $\tilde{q}_2(y)$:

$$\tilde{q}_2(y) = \frac{\gamma}{\omega^{2-\alpha}}(y+1)^{1-\alpha/2}. \tag{C4}$$

The crossings of $\tilde{q}_{1\pm}(y)$ and $\tilde{q}_2(y)$ determine the extremal points of $\chi''(\Omega)$, and using the fact that for $y \to \infty$ $\tilde{q}_2(y) \propto y^{1-\alpha/2}$ and $\tilde{q}_{1\pm}(y) \propto y$, we have six different scenarios for the crossing of $\tilde{q}_2(y)$ and $\tilde{q}_{1\pm}(y)$: (i) $\tilde{q}_2(y)=\tilde{q}_{1-}(y)$ for a single y and there are no other crossings; (ii) $\tilde{q}_2(y_1)=\tilde{q}_{1-}(y_1)$ and $\tilde{q}_2(y_2)=\tilde{q}_{1+}(y_2)$ for $y_1<y_2$; (iii) $\tilde{q}_2(y_1)=\tilde{q}_{1-}(y_1)$, $\tilde{q}_2(y_2)=\tilde{q}_{1+}(y_2)$, and $\tilde{q}_2(y_3)=\tilde{q}_{1+}(y_3)$ for $y_1<y_2<y_3$; (iv) $\tilde{q}_2(y_1)=\tilde{q}_{1+}(y_1)$, $\tilde{q}_2(y_2)=\tilde{q}_{1+}(y_2)$, and $\tilde{q}_2(y_3)=\tilde{q}_{1+}(y_3)$ for $y_1<y_2<y_3$; (v) $\tilde{q}_2(y_1)=\tilde{q}_{1+}(y_1)$ and $\tilde{q}_2(y_2)=\tilde{q}_{1+}(y_2)$ for $y_1<y_2$; and (vi) $\tilde{q}_2(y)=\tilde{q}_{1+}(y)$ for a single y and there are no other crossings.

Generally if there is only one crossing, scenarios (i) and (vi), the meaning is that $\chi''(\Omega)$ will have only one maximum; on the contrary, when there are three crossings, scenarios (iii) and (iv), there are two maxima and one minimum for $\chi''(\Omega)$. These correspond to two different phases the one-peak and the double-peak phase, where the scenarios (ii) and (v) are the boundaries between these phases. We are interested in finding these boundaries, where for scenario (ii) and (v) two conditions must be satisfied:

$$\tilde{q}_2(y_1) = \tilde{q}_{1+}(y_1) \tag{C5}$$

and

$$\left.\frac{d\tilde{q}_2(y)}{dy}\right|_{y=y_1} = \left.\frac{d\tilde{q}_{1+}(y)}{dy}\right|_{y=y_1}. \tag{C6}$$

Starting from Eq. (C5) we compare the left-hand side to some constant $\tilde{c}$ and using Eq. (C4) we find

$$y = \tilde{c}^{2/(2-\alpha)}\frac{\omega^2}{\gamma^{2/(2-\alpha)}} - 1. \tag{C7}$$

Comparing the right hand side of Eq. (C5) to the same $\tilde{c}$ and using Eq. (C7) we arrive at the relation

$$\left(\frac{\omega}{\gamma^{1/(2-\alpha)}}\right)^2 = \left[1 - \frac{2}{\alpha} + \frac{1}{2}\sqrt{\frac{16}{\alpha^2} - 4\left(\frac{4\cos(\pi\alpha/2)}{\alpha}\tilde{c} - \tilde{c}^2\right)}\right]\tilde{c}^{-2/(2-\alpha)}. \tag{C8}$$

Next, performing the derivation in Eq. (C6) and using Eq. (C7) we find

$$\left(\frac{\omega}{\gamma^{1/(2-\alpha)}}\right)^2 = \left\{\frac{1}{2} - \frac{1}{\alpha} + \frac{1}{2}\sqrt{\frac{(4-2\alpha)^2}{4\alpha^2} + \tilde{c}\left(\frac{2-\alpha}{\alpha}\right)\left[2\alpha\tilde{c} - 4\cos\left(\frac{\pi\alpha}{2}\right)\right]}\right\}\tilde{c}^{-2/(2-\alpha)}. \tag{C9}$$

Comparison of Eqs. (C8) and (C9) supplies an equation for $\tilde{c}$:

$$4\alpha^2\tilde{c}^4 - 16\cos\left(\frac{\pi\alpha}{2}\right)(2+\alpha)\tilde{c}^3 + \frac{16}{\alpha^2}\left[-4 + 8\alpha - \alpha^2 + \cos^2\left(\frac{\pi\alpha}{2}\right)(2+\alpha)^2\right]\tilde{c}^2 - \frac{64}{\alpha^2}\cos\left(\frac{\pi\alpha}{2}\right)(6-\alpha)\tilde{c} + \frac{64}{\alpha^3}(4-\alpha) = 0. \tag{C10}$$

Equation (C10) is a fourth-order polynomial and could be solved by standard methods or using MATHEMATICA. It has four different solutions of which two have nonzero imaginary parts for any $0<\alpha<1$, while the other two have no imaginary part for $\alpha<\alpha_{\chi_2}\approx 0.70776$. Let us call these solutions $\tilde{c}_1(\alpha)$ and $\tilde{c}_2(\alpha)$. A nonzero imaginary part for $\alpha>\alpha_{\chi_2}$ of both $\tilde{c}_1(\alpha)$ and $\tilde{c}_2(\alpha)$ means that only scenario (vi) is applicable for such α's and we are in the one-peak phase. The boundaries between the two phases are given by

$$\frac{\omega}{\gamma^{1/(2-\alpha)}} = \tilde{g}_{1,2}(\alpha) = \sqrt{1 - \frac{2}{\alpha} + \frac{1}{2}\sqrt{\frac{16}{\alpha^2} - 4\left(\frac{4\cos(\pi\alpha/2)}{\alpha}\tilde{c}_{1,2}(\alpha) - \tilde{c}_{1,2}^2(\alpha)\right)}}\,\tilde{c}_{1,2}^{-1/(2-\alpha)}(\alpha), \tag{C11}$$

where the subscript 1 is for the lower bound $\tilde{g}_1(\alpha)$ and subscript 2 is the upper bound $\tilde{g}_2(\alpha)$ in Fig. 12. For $\tilde{g}_1(\alpha)$ there is also another interesting point $\alpha_{\chi_1}=0.527\,031$ which satisfies the following relation:

$$\alpha_{\chi_1}^2 - 4\alpha_{\chi 1} + 4\cos^2\left(\frac{\pi\alpha_{\chi_1}}{2}\right) = 0, \tag{C12}$$

for $\alpha<\alpha_{\chi_1}$, $\tilde{g}_1(\alpha)=0$.

[1] S. A. Adelman, J. Chem. Phys. **64**, 124 (1976).
[2] E. Lutz, Phys. Rev. E **64**, 051106 (2001).
[3] R. Morgado, F. A. Oliveira, G. G. Batrouni, and A. Hansen, Phys. Rev. Lett. **89**, 100601 (2002).
[4] N. Pottier, Physica A **317**, 371 (2003).
[5] S. Chaudhury and B. J. Cherayil, J. Chem. Phys. **125**, 024904 (2006).
[6] J. D. Bao, P. Hänggi, and Y. Z. Zhuo, Phys. Rev. E **72**, 061107 (2005).
[7] R. Kupferman, J. Stat. Phys. **114**, 291 (2004).
[8] I. Goychuk and P. Hänggi, Phys. Rev. Lett. **99**, 200601 (2007).
[9] R. Metzler and J. Klafter, Phys. Rep. **339**, 1 (2000).
[10] H. Yang, G. Luo, P. Karnchanaphanurach, T. Louie, I. Rech, S. Cova, L. Xun, and X.S. Xie, Science **302**, 262 (2003).
[11] W. Min, G. Luo, B. Cherayil, S. Kou, and X. Xie, Phys. Rev. Lett. **94**, 198302 (2005).
[12] T. W. Kibble and F. H. Berkshire, *Classical Mechanics* (Longman, London, 1996).
[13] A. D. Viñales and M. A. Despósito, Phys. Rev. E **73**, 016111 (2006).
[14] S. Burov and E. Barkai, Phys. Rev. Lett. **100**, 070601 (2008).
[15] B. Mandelbrot and J. Van Ness, SIAM Rev. **10**, 422 (1968).
[16] H. Qian, in *Processes with Long-Range Correlations: Theory and Applications*, edited by G. Rangarajan and M. Z. Ding, Lecture Notes in Physics Vol. 621 (Springer, New York, 2003), p. 22.
[17] S. C. Kou and X. S. Xie, Phys. Rev. Lett. **93**, 180603 (2004).
[18] Fractional Gaussian noise is usually defined by [16] $\langle \xi(\tau)\xi(t)\rangle \propto 2H(2H-1)|t-\tau|^{2H-2}+2H|t-\tau|^{2H-1}\delta(t-\tau)$, where H is the Hurst exponent and is related to α by $\alpha=2-2H$. For $0<\alpha<1$ the second term on the right has no effect and we get Eq. (3).
[19] R. Kubo, M. Toda, and N. Hashitsume, *Statistical Physics II, Nonequilibrium Statistical Mechanics* (Springer-Verlag, Berlin, 1985).
[20] S. G. Samko, A. A. Kilbas, and O. I. Marichev, *Fractional Integrals and Derivatives and Their Applications* (Nauka i Technika, Minsk, 1987) (in Russian).
[21] K. S. Miller and B. Ross, *An Introduction to the Fractional Differential Equations* (Wiley, New York, 1993).
[22] J. M. Porrà, K. G. Wang, and J. Masoliver, Phys. Rev. E **53**, 5872 (1996).
[23] R. Zwanzig, J. Stat. Phys. **9**, 215 (1973).
[24] E. Barkai and R. J. Silbey, J. Phys. Chem. **104**, 3866 (2000).
[25] I. M. Sokolov, J. Klafter, and A. Blumen, Phys. Today **55** (11), 48 (2002).
[26] E. Katzav, M. Adda-Bedia, and B. Derrida, Europhys. Lett. **78**, 46006 (2007).
[27] E. Barkai, Phys. Rev. E **63**, 046118 (2001).
[28] R. Metzler, E. Barkai, and J. Klafter, Phys. Rev. Lett. **82**, 3563 (1999).
[29] B. N. Narahari Achar, J. W. Hanneken, T. Enck, and T. Clarke, Physica A **297**, 361 (2001).
[30] Ya. E. Ryabov and A. Puzenko, Phys. Rev. B **66**, 184201 (2002).
[31] G. M. Zaslavsky, A. A. Stanislavsky, and M. Edelman, Chaos **16**, 013102 (2006).
[32] A. A. Kilbas, H. M. Srivastava, and J. J. Trujillo, *Theory and Applications of Fractional Differential Equations* (Elsevier, Amsterdam, 2006).
[33] According to Ref. [32], such a fractional oscillator was considered by F. Mainardi, in *Proceedings of the 12th IMACS World Congress, Atlanta, 1994*, edited by W. F. Ames (GeorgiaTech, Atlanta, 1994), Vol. 1, pp. 329–333.
[34] M. A. Lavrentiev and B. V. Shabat, *Methods of the Theory of Functions of Complex Variables* (Nauka, Moscow, 1973).
[35] G. Doetsch, *Guide to the Applications of Laplace Transforms* (Van Nostrand, London, 1961).
[36] *Handbook of Mathematical Functions with Formulas, Graphs, and Mathematical Tables*, edited by M. Abramowitz and I. Stegun (Dover, New York, 1971).
[37] A. Erdèlyi, *Tables of Integral Transforms* (McGraw-Hill, New York, 1954).
[38] W. Feller, *An Introduction to Probability Theory and Its Applications* (John Wiley and Sons, New York, 1971), Vol. 2.
[39] F. Barbi, M. Bologna, and P. Grigolini, Phys. Rev. Lett. **95**, 220601 (2005).
[40] I. M. Sokolov and J. Klafter, Phys. Rev. Lett. **97**, 140602 (2006).
[41] E. Heinsalu, M. Patriarca, I. Goychuk, and P. Hänggi, Phys. Rev. Lett. **99**, 120602 (2007).
[42] K. Weron and M. Kotulski, Physica A **232**, 180 (1996).
[43] I. Goychuk, Phys. Rev. E **76** 040102(R) (2007).
[44] R. Granek and J. Klafter, Phys. Rev. Lett. **95**, 098106 (2005).
[45] G. Luo, I. Andricionoaei, X. S. Xie, and M. Karplus, J. Phys. Chem. B **110**, 9363 (2006).
[46] W. T. Coffey, Yu. P. Kalmykov, and S. V. Titov, Phys. Rev. E **65**, 032102 (2002).
[47] W. T. Coffey, Yu. P. Kalmykov, and S. V. Titov, Phys. Rev. E **65**, 051105 (2002).
[48] W. T. Coffey, Yu. P. Kalmykov, and J. T. Waldron, *The Langevin Equation: With Applications to Stochastic Problems in Physics, Chemistry, and Electrical Engineering* (World Scientific, Hackensack, 2004).
[49] M. Y. Rocard, J. Phys. Radium **4**, 247 (1933).
[50] B. K. P. Scaife, *Principles of Dielectrics* (Oxford University Press, London, 1989).
[51] E. Dachwitz, F. Parak, and M. Stockhausen, Ber. Bunsenges. Phys. Chem **93**, 1454 (1989).
[52] W. Götze and L. Sjörgen, Rep. Prog. Phys. **55**, 241 (1992).
[53] N. Nandi and B. Bagchi, J. Phys. Chem. A **102**, 8217 (1998).